

THE INVESTIGATION OF FEED EFFECTS IN TOOL-LIFE TESTS WITH RADIOACTIVE TOOLS

By
S. B. DATAR

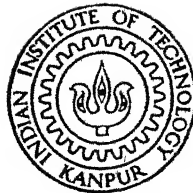
ME ^{FH} 1977/11
T-262i

1977

M

DAT

INV



DEPARTMENT OF MECHANICAL ENGINEERING
INDIAN INSTITUTE OF TECHNOLOGY, KANPUR
DECEMBER, 1977

THE INVESTIGATION OF FEED EFFECTS IN TOOL-LIFE TESTS WITH RADIOACTIVE TOOLS

A Thesis Submitted
In Partial Fulfilment of the Requirements
for the Degree of
MASTER OF TECHNOLOGY

00000

By
S. B. DATAR

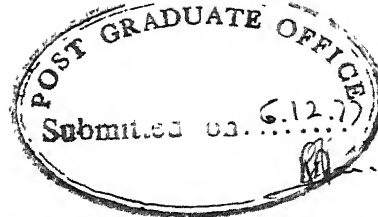
to the
DEPARTMENT OF MECHANICAL ENGINEERING
INDIAN INSTITUTE OF TECHNOLOGY, KANPUR
DECEMBER, 1977

LIBRARY
CENTRAL LIBRARY

Acc. No. A 54003

1973

ME-1977-M-DAT-INV



ii

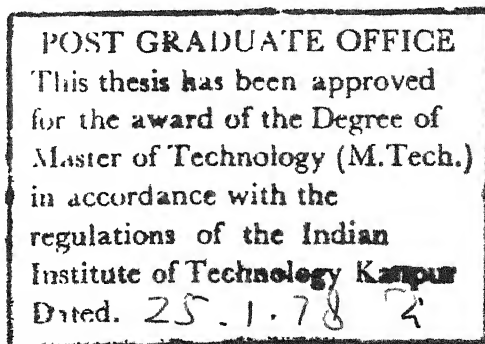
CERTIFICATE

Certified that the present work entitled 'The Investigation of Feed Effects in Tool-life Tests with Radioactive Tools', has been carried out by Mr. S.B. Datar under my supervision and has not been submitted elsewhere for the award of a degree.

Rakesh Chawla

(R. Chawla)
Assistant Professor
Department of Mechanical Engineering
Indian Institute of Technology,
Kanpur

December, 1977



ACKNOWLEDGEMENTS

This thesis would not have achieved its final form but for those who so willingly gave of their time and energy. First and foremost, I thank Dr. R. Chawla for sincere guidance, encouragement and criticism at all stages of this work. I am thankful to Dr. G.K. Lal for valuable suggestions and comments.

I wish to express my heartiest appreciation to Mr. N. Sridharan (Design Engineer, Larson and Toubro Co., Bombay) for generous help and understanding support throughout the course of this work.

Sincere thanks are also due to many people at IIT Kanpur, in particular to Mr. S.S. Pathak, Mr. R.M. Jha, Mr. B.P. Vishwakarma for technical support, to Mr. J.D. Verma for excellent typing and to Mr. D.K. Nishra for tracing work.

Financial assistance is gratefully acknowledged from the Department of Atomic Energy, Govt. of India, under whose sponsorship this work has been carried out.

S.B. Datar

CONTENTS

<u>Chapter</u>		<u>Page</u>
I	INTRODUCTION	1
II	GENERAL REVIEW	
	2.1 Tool-life criteria and equations	
	2.1.1 Tool-life	4
	2.1.2 Tool-life equations	5
	2.2 Tool-life testing	7
	2.2.1 Direct testing	8
	2.2.2 Accelerated tests	8
	2.3 Radioactive tool-life testing	9
	2.3.1 Determination of Absolute tool wear	10
	2.3.2 Separation of Flank wear and Crater wear	11
	2.3.3 Testing techniques	12
III	TESTING METHODS	
	3.1 Multifeed testing	14
	3.2 Extension of multispeed testing for obtaining feed parameters	16
	3.3 Deduction of Flank and Crater wear from Total wear measurements	19
	3.3.1 Assumptions made	20
	3.3.2 Determination of a and b	23
IV	EXPERIMENTAL PARTICULARS	
	4.1 Cutting tools and work material	26
	4.2 The lathe and counting set-ups	27
	4.3 Experimental procedures	
	4.3.1 Deduction of Absolute wear volumes	28
	4.3.2 Multifeed tests	29
	4.3.3 Extension of multispeed testing	30

<u>Chapter</u>		<u>Page</u>
	4.3.4 Conventional tests	30
	4.3.5 Validation of the proposed method for Flank and crater separation	31
V	RESULTS AND DISCUSSIONS	
	5.1 Multifeed Tests	33
	5.1.1 Tool-life values obtained from multifeed tests	34
	5.1.2 Feed parameters from multifeed tests	35
	5.2 Multispeed tests	35
	5.2.1 Tool-life values obtained from multispeed tests	36
	5.2.2 Feed parameters from multispeed tests	38
	5.3 Conventional tests	39
	5.4 Comparison of feed parameters from multifeed, multispeed and conventional tests	40
	5.5 Deduction of flank and crater wear xxx volumes from total wear volume measurements	
	5.5.1 Single speed/feed test	41
	5.5.2 Multifeed Test 3	43
	5.5.3 Multifeed Test 2	46
	5.5.4 Other Tests	46
VI	CONCLUSIONS AND SCOPE FOR FURTHER WORK	
	6.1 Conclusions	51
	6.2 Scope for further work	52
	REFERENCES	54

LIST OF TABLES

Table

- 5.1: Cutting conditions for multifeed tests.
- 5.2: Tool-life values from multifeed tests.
- 5.3: Average n_2, C_2 values from multifeed tests.
- 5.4: Cutting conditions for multispeed tests.
- 5.5: Tool-life values from multispeed tests.
- 5.6: Average n_1, C_1 values from multispeed tests.
- 5.7: Average n_2, C_2 values from multispeed tests.
- 5.8: Cutting conditions for conventional tests.
- 5.9: Comparison of n_2, C_2 values obtained from multifeed, multispeed and conventional tests.
- 5.10: Cutting conditions for single speed/feed test.
- 5.11: Comparison of deduced and actual a, b values in SSF.
- 5.12: Comparison of tool-life values from a, b values with the actual tool-life values in SSF.
- 5.13: Cutting conditions for multifeed test 3.
- 5.14: Comparison of deduced a, b values in MF3 with actual a, b values of MF1.

Table

- 5.15: Comparison of tool-life values from a,b values in MF3 with actual tool-life values from MF1 and MF3.
- 5.16: Comparison of deduced and actual a,b values in MF2.
- 5.17: Comparison of deduced and actual a,b values in OT1.
- 5.18: Comparison of tool-life values from a,b values with actual tool-life values in OT1.
- 5.19: Comparison of deduced and actual a,b values in OT2.
- 5.20: Comparison of tool-life values from a,b values with actual tool-life values in OT2.

LIST OF FIGURES

Figure

- 3.1: Growth of flank wear-land.
- 3.2: Inverse wear-land growth rate curves.
- 3.3: Geometry of tool-wear.
- 3.4: Effect on tool-lives with (a) Total volume criterion, (b) Crater volume criterion.
- 4.1: Radiation levels in mR/hr during the machining tests.
- 4.2: Block diagram of the counting set-up.
- 5.1: Inverse wear-land growth rate curves for multifeed test 1.
- 5.2: Inverse crater volume growth rate curves for multifeed test 1.
- 5.3: Inverse total wear volume growth rate curves for multifeed test 1.
- 5.4: Inverse wear-land growth rate curves for multifeed test 2.
- 5.5: Inverse crater volume growth rate curves for multifeed test 2.
- 5.6: Inverse total wear volume growth rate curves for multifeed test 2.

Figure

- 5.7: Inverse wear-land growth rate curves for multispeed test 1.
- 5.8: Inverse crater volume growth rate curves for multispeed test 1.
- 5.9: Inverse total wear volume growth rate curves for multispeed test 1.
- 5.10: Inverse wear-land growth rate curves for multispeed test 2.
- 5.11: Inverse crater volume growth rate curves for multispeed test 2.
- 5.12: Inverse total-wear volume growth rate curves for multispeed test 2.
- 5.13: Conventional measurements of wear-land growth in orthogonal cutting.
- 5.14: Wear growth curves for the work material.
- 5.15: Inverse wear-land growth rate curve for single speed/feed test.
- 5.16: Inverse crater volume growth rate curve for single speed/feed test.
- 5.17: Inverse total wear volume growth rate curve for single speed/feed test.
- 5.18: (a) Wear-rate and (b) Square-of-wear-rate curves for single speed/feed test.

Figure

- 5.19: Square-of-wear-rate curves for multifeed test 3.
- 5.20: Inverse total wear volume growth rate curves for multifeed test 3.
- 5.21: Square-of-wear-rate curves for multifeed test 2.
- 5.22: Inverse wear growth rate curves (a) crater wear volume and (b) flank wear land, of a set in other test 1.
- 5.23: Square-of-wear-rate curves for other test 1.
- 5.24: Wear-rate curve for other test 2.
- 5.25: Square-of-wear-rate curve for other test 2.

Plate:

- 1: General view of the experimental set-up.

ABSTRACT

Feed effects on tool-life parameters are investigated by using radioactive tools, ^{60}Co being the radiotracer. Orthogonal cutting conditions (using tubes) were achieved, to obtain repeatable and unambiguous results. Feed parameters obtained by multifeed testing were compared with those obtained by extending multispeed tests and conventional tests (using microscope). A novel method which gives the behaviour of crater and flank wear from certain considerations of the total wear volume measurements has been proposed and some experimental validation was achieved. For the tool/work combination investigated, the proposed method gave reasonable results. It is shown that more reliable results may be obtained if the inverse wear-rate curves are better defined.

CHAPTER I

INTRODUCTION

The need for accurate, rapid assessment of tool life has become more crucial in recent years, with the development of numerically controlled machine-tools and the increased application of various optimization techniques. The usual approach is the determination of certain constants, which define an appropriate equation relating tool life to the machining variables involved. For some industrial applications, discrete values of tool-life may be preferred to tool life equations. However, for a general evaluation of economic conditions, there are obvious advantages in using a suitable equation.

Conventional methods for tool-life testing require a great deal of time and material, considerable costs being involved in obtaining a relatively small amount of tool-life data. Accelerated tests have been suggested, but these do not always yield comprehensive results. In any case, the low sensitivity of conventional measuring techniques, e.g. microscopical measurements of wear-land width, remains a basic limitation in such tests.

A number of investigators [1 - 6] have reported the application of nuclear techniques for tool-life testing using radioactive tools (Sec. 2.3). High sensitivity

is the characteristic feature of nuclear methods, and this may be illustrated by two recently reported, on-line applications of nuclear techniques to production processes. Thus, Askouri, et. al [7] used surface-activated dies to enable the direct monitoring of die wear in wire drawing, under normal industrial conditions. On-line control of process parameters was shown to be possible in principle, something impossible to achieve if one uses conventional measuring techniques, e.g. micrometer measurements of the diameter of the drawn wire. Another illustrative example is the micro-isotope technique reported by Cook et. al [8] for tool-wear sensing in numerically controlled machines. A microscopic amount of a radioisotope is brazed onto a particular point of the cutting tool, e.g., at a point on the clearance face corresponding to a particular wear-land criterion. When, in the process of cutting, the micro-isotope is carried away by the chips, a sensor focussed on the tool suddenly records zero activity and an appropriate instruction signal is fed to the machine.

In the present work, the high sensitivity of nuclear technique has been exploited for the development of rapid tool-life testing methods for studying feed effects, under controlled laboratory conditions. One proposed method is the multifeed approach, wherein the same cutting edge of a radioactive tool is used to generate

tool-life data for a number of discrete feed values. A second method extends the scope of multispeed testing [19], wherein data from a suitable set of multispeed tests is used to deduce the effects of feed. A novel approach has also been presently suggested for the separation of flank and crater contributions to total wear, and this has been applied in a test for deducing feed effects on flank and crater wear separately, through, measurements of total wear volume alone. Comparisons of results for the nuclear tests have been made with the conventional methods for the case of wear-land width (flank) criterion.

Chapter II is a brief general review of tool-life evaluation. The presently proposed methods are described in Chapter III. Chapter IV gives relevant experimental particulars. Results are presented and discussed in Chapter V, while the final Chapter gives the conclusions and indicates the scope for further work.

CHAPTER II

GENERAL REVIEW

2.1: Tool Life Criteria and Equations

2.1.1: Tool Life

From a functional point of view, the life of a cutting tool is the duration for which it can be employed in the production of 'satisfactory' parts. It can be taken as, the period of time for which the tool can be used before resharpener or replacement is necessitated. Tool life can be defined in a number of ways, depending upon one of the following criteria.

1. Tool-failure:

A tool is considered to have failed when it either fails to cut or cuts in a manner grossly different from that of a sharp tool. Tool failure is generally the proper tool-life criteria when roughing is considered, i.e. where tolerance or finish is not required. Tool failure is specified as follows:

- i) Wear-land size on the clearance face.
- ii) Crater depth or crater volume on the rake face.
- iii) Total volume, or weight, of material worn off the tool.
- iv) Combination of (i) and (ii)
- v) Chipping or fine cracks developing on the cutting edge, etc.

2. Workpiece dimensional tolerances:

This criterion is useful when form tools are used, in preset tooling and in various automatic operations. The tool is replaced when the dimensions of the workpiece lie outside the specified tolerances.

3. Surface finish degradation:

For finishing cuts, or pre-grind cuts, the deterioration of surface finish can be a more meaningful criterion for tool life.

The tool life value, T , for a given operation will depend on the type of criterion used, and it is therefore essential that this be explicitly stated. Thus, for example, a possible criterion for roughing cuts with a cemented carbide tool, may be a wear-land width, l_w , of 0.75 mm., and the tool-life would then be defined as the cutting time for attaining this.

2.1.2 Tool-life equations:

The cutting speed, V , usually has the dominating effect on tool life. According to Taylor's tool-life relationship [9], one has, for a given range of cutting conditions

$$VT^{n_1} = C_1 \quad (2.1)$$

where n_1 is a constant speed exponent and C_1 is a constant coefficient.

Cook [10], in a recent review, has shown that feed (f) and depth of cut (d) effects are conveniently taken into account by considering an equation of the form

$$T = k V^{-1/n_1} f^{-1/n_2} d^{-1/n_3} \quad (2.2)$$

where n_2 and n_3 are constant exponents for feed and depth of cut, respectively, and k is another constant. This is again, applicable for a given tool/work material combination, over a given range of cutting conditions. The equation has been used by a number of workers and found to yield satisfactory agreement with experimental data.

More generalised tool-life equation have been suggested by other investigators. For example, Kronenberg [11] derived an equation from dimensional analysis, in which the effect of work material properties, cutting tool temperature, etc. are incorporated.

Trigger [12] related the tool-life to cutting tool temperature through a simple relation

$$T = \text{const } \theta^{-\beta} \quad (2.3)$$

where θ is the temperature and β is a constant temperature exponent.

Colding [13] developed a three-dimensional tool life equation, by introducing the concept of a chip equivalent, q , as the ratio of engaged cutting length and the area of cut.

Uehara [14] proposed a relationship between tool-life and total wear volume of the form

$$W = \alpha T^{\beta} \quad (2.4)$$

where W is the total wear volume, and α , β are constants. This equation was considered for investigating the compatibility of results from certain short-time tool life tests, such as radioactive tests, and those from conventional ones.

For the proposed work, with the principal investigation being of feed effects, Equation (2.2) was modified to the Taylor-type equation

$$\text{i.e. } f T^{n_2} = C_2 \quad (2.5)$$

where n_2 is the feed exponent as before, and C_2 is a constant.

2.2 Tool Life Testing

Tool-life testing is carried out for obtaining the various constants characterising a particular type of tool-life equation. This is then used for the selection of

optimum cutting conditions for a particular operation. Tool-life tests can be carried out in a number of ways, the conventional methods being reviewed below.

2.2.1 Direct testing:

The most direct way to obtain tool-life data is to perform a test until the chosen criterion is reached. This has to be done at different cutting speeds, feeds, depths of cut, etc., varying only one parameter at a time. This obviously becomes a tedious process, considering that tool-life values may be typically 50 - 100 minutes.

2.2.2 Accelerated tests:

Accelerated conventional tests for tool life have been reported by various workers for affecting savings in testing time and material consumed. It has been shown [15] that, the scatter in tool-life data thus obtained is similar to that for direct methods. In the simplest type of accelerated test, tool wear, etc., is extrapolated to a specified failure criterion after carrying out a direct type test for a shorter duration. Other types of accelerated tests, for obtaining the constants in Taylor equation (Eqn. 2.1), include:

- i) Facing test [16]
- ii) Taper turning test [17]

and iii) Variable-rate machining test [18]

The above tests are for the determination of speed parameters only, there being no available accelerated tests to study feed effects - the primary objective for the present work.

2.3: Radioactive Tool-Life Testing

Tool-life tests with radioactive tools are particularly useful in obtaining tool-life data in a more expedient manner. Conventional tests cannot be accelerated beyond a certain limit because of the low sensitivity of the wear sensing techniques, e.g. microscopic measurements. The use of radioactive tools for measuring wear, on the other hand, provides sufficiently high sensitivity for obtaining even the instantaneous rate of tool wear at any given time. This is determined by measuring the radioactivity of the mass of chips collected during a brief time of cutting.

Several investigators have examined the radioactive technique over the past two decades. Merchant [1, 2] showed that 95% of the worn particles from the cutting tool adhere to the chips even in wet-cutting. Much of the earlier work was done by employing Geiger - Muller counting of β or γ radiation for obtaining the total volumetric wear of the cutting tool. More recently, Na I counters have been employed for γ counting of the chip samples.

2.3.1 Determination of absolute tool wear

The absolute amount of tool material transferred to the chips can be obtained in a number of ways, viz.

i) The specific activity of the tool bits is calculated from irradiation and nuclear data. The counter efficiency is determined separately, so that, the absolute activity of the chip samples can be computed [2]. This method obviously has serious sources of systematic errors.

ii) A weighed piece of tool material is irradiated together with the tool bit. The reference sample is dissolved in a suitable chemical agent. A known part of its activity is measured under identical counting conditions (geometry, etc.) as used for measurements with chip samples [3]. This procedure is naturally painstaking and necessitates the handling of liquid samples. Besides, finite differences in counting geometry can lead to large errors in normalizing the results.

iii) The radiotracer is chemically separated from the weighed piece of tool material, as well as, from a given chip sample. The two activities are compared using liquid scintillation counting techniques [4]. The chemistry involved here is obviously tedious.

iv) More recently, $\gamma - \gamma$ coincidence counting of a suitable radiotracer, viz. ^{60}Co , has been applied by Chawla

and Bhattacharya [6] for deducing absolute wear volumes for irradiated H.S.S. tools. Here, the need for explicit consideration of the counting geometry and efficiency is completely eliminated in the comparison of the activities of a chip sample and the reference piece of tool material. It is this normalising method which has been employed in the present work.

2.3.2 Separation of flank and crater wear

For the separation of flank and crater wear volumes in radioactive tool life testing, two methods have been used in the past. The first is applicable to β counting only, and involves counting of β radiation from the smoother surface of the chips separately from the counting of the rough surface. The former counts are due to wear particles from the rake face, i.e. crater, and the latter to particles from the clearance face, i.e. flank.

The more popular method of separating flank and crater effects is that of Hake and Opitz [5], wherein two tools are used to cut simultaneously on opposite sides of the workpiece. One tool is the radioactive test tool, while the second is an unirradiated tool. Chips produced by the test tool have activated particles from the rake face attached to them, while chips produced by the non-activated tool contain active particles from the clearance face of the test tool.

In the present work with γ counting being employed, the Hake and Opitz method was applied for most of the experiments. However, a method has been presently proposed and verified for deducing flank and crater volumes simply from certain considerations of the total volumetric wear rate (Sec. 3.3).

2.3.3 Testing techniques

Cook and Lang [5], indicated certain difficulties in obtaining reliable, quantitative results from short tool-life tests with radioactive tools. However, such **criticism** has been principally of the methods employed and not of the potential accuracy that can be achieved.

Chawla and Bhattacharya [19] have recently shown that, with proper precautions being taken, radioactive tool-life testing can be successfully applied to provide significant savings in testing time and materials over conventional methods, while providing reliable results. For deducing the parameters, n_1 and C_1 , in Taylor's equation (Eqn. 2.1) a multispeed testing approach was proposed, whereby a single cutting edge was used to simultaneously yield tool-life data for a number of discrete **cutting** speeds. This was done by suitable interpolation of the instantaneous rates of absolute wear measured at different stages of a single multispeed test with the radioactive tool.

In the present work, it has been shown that tool life parameters for feed effects, viz. n_2 and C_2 in Eqn.(2.5), can be reliably obtained from either

- i) A single multifeed test carried out at constant speed.
- or ii) A set of multispeed tests, each carried out with different feed.

CHAPTER III

TESTING METHODS

3.1: Multifeed Testing

As discussed in Section 2.3, radiotracer techniques provide sufficiently high sensitivity for the determination of instantaneous rates of tool wear. The presently proposed multifeed method exploits this feature for the determination of the feed constants n_2 and C_2 of Equation (2.5), in a manner similar to that used in multispeed testing for the study of speed effects [19].

Typical growth of wear-land width with cutting time is shown in Fig. 3.1, from which may be observed certain characteristic features. Considering the curve corresponding to feed f_2 , Region 1, upto point P, denotes the zone of initial 'break in'. In this region, the initially sharp cutting edge wears rapidly due to plastic deformation and consequential temperature rise. After B, the tool wears in a uniform manner till the point C is reached. The region B - C, Region 2, is the mechanical wear region, viz. wear region under temperature insensitive conditions. Beyond C, the wear-land grows rapidly and the tool fails soon thereafter. The same features characterise the curve that would be obtained for a higher (f_3), or lower (f_1), feed value, the cutting speed being kept constant (Fig. 3.1).

It is seen that, for a given failure criterion of wear-land width, w_f , one would obtain tool lives T_1, T_2, T_3 , corresponding to feeds f_1, f_2 and f_3 , respectively. These pairs of f_i, T_i values could then be used for obtaining the feed parameters n_2, C_2 of Equation (2.5.).

In the proposed multifeed method, one basically adopts the inverse wear-rate approach used for multispeed testing [19]. The plots considered are $\frac{dt}{dw}$ - vs - w , where $\frac{dt}{dw}$ is the reciprocal of the wear rate and w is the cumulative wear. With this representation, the wear growth curves corresponding to feeds f_1, f_2, f_3 are of the type shown in Fig. 3.2 and the same three characteristic regions may be identified. In particular the constant wear-rate region, Region 2, of Fig. 3.1 becomes a "plateau" in Fig. 3.2.

From Fig. 3.2, it can be inferred that the tool life corresponding to a given failure criterion w_f and a given feed f_i , will be the area under the appropriate inverse wear-rate curve, since

$$T_i = \int_0^{w_f} \left(\frac{dt}{dw} \right)_i dw \quad (3.0)$$

Thus for example, T_2 is the area under the f_2 curve as indicated by the shaded area in Fig. 3.2

The inverse wear-rate curves for different feeds can be generated in a single test with a radioactive tool

by changing the feed between machining intervals. Simultaneous generation of the (f_i, T_i) pairs required for determining n_2, C_2 would thus be achieved. The basic assumption, as in the case of multispeed testing, is that the instantaneous wear rate at any stage depends only on the tool's current cutting conditions and not on its past history. This assumption was shown to be valid for the present experiments by carrying out a single speed/feed test and comparing the wear growth curves with results from the corresponding multifeed test.

3.2: Extension Of Multispeed Testing For Obtaining Feed Parameters

Consider the more general tool-life equation, Equation (2.2), viz.

$$T = k V^{-1/n_1} f^{-1/n_2} d^{-1/n_3}$$

With depth of cut effects absent, one may write this in the form

$$T = K V^{-1/n_1} f^{-1/n_2} \quad (3.1)$$

In multispeed testing [19], one determines the speed parameters n_1, C_1 , of Taylor's equation, Equation (2.1), viz.

$$VT^{n_1} = C_1$$

Such a test would then be carried out at a constant value of feed, say f_1 , and one may rewrite the

Taylor equation as

$$T = (C_1)_{f_1}^{1/n_1} V^{-1/n_1} \quad (3.2)$$

where $(C_1)_{f_1}$ denotes the speed constant C_1 , corresponding to a feed value of f_1 .

Comparing Equations (3.1) and (3.2),

$$K f_1^{-1/n_2} = (C_1)_{f_1}^{1/n_1} \quad (3.3)$$

If a multispeed test is carried out over the same speed range but for a different feed, say f_2 , one would obtain the same speed exponent n_1 (assumed independent of feed from the very nature of Equation (3.1)), but a new value of C_1 , viz $(C_1)_{f_2}$. The latter would be related to f_2 by an equation similar to Equation (3.3), i.e.,

$$K f_2^{-1/n_2} = (C_1)_{f_2}^{1/n_1} \quad (3.4)$$

It will now be shown that the above pair of multispeed tests, carried out for feeds f_1 and f_2 , may be used to obtain the feed constant n_2 , C_2 of the Taylor-type equation, Equation (2.5), viz.

$$f T^{n_2} = C_2$$

Dividing Equation (3.3) by Equation (3.4)

$$\left(\frac{f_1}{f_2} \right)^{-1/n_2} = \left[\frac{(C_1)_{f_1}}{(C_1)_{f_2}} \right]^{1/n_1} \quad (3.5)$$

Taking logs of both sides,

$$-\frac{1}{n_2} \log \left(\frac{f_1}{f_2} \right) = \frac{1}{n_1} \log (C_1)_{f_1} / (C_1)_{f_2}$$

or

$$n_2 = n_1 \frac{\log (f_2/f_1)}{\log (C_1)_{f_1} / (C_1)_{f_2}} \quad (3.6)$$

All the quantities on the R.H.S are known from the pair of multispeed tests, so that n_2 may be computed.

For obtaining the second feed parameter, C_2 in Equation (2.5), we may determine the value of this corresponding to the intermediate speed in the multispeed (V_1, V_2, V_3) tests, say V_2 . From Equation (3.2), the tool-life value for speed V_2 and feed f_1 is given by

$$T_{21} = (C_1)_{f_1}^{1/n_1} V_2^{-1/n_1} \quad (3.7)$$

The same tool-life may be expressed in terms of f_1 , using Equation (2.5), i.e.,

$$T_{21} = (C_2)_{V_2}^{1/n_2} f_1^{-1/n_2} \quad (3.8)$$

From Equations (3.7), (3.8),

$$(C_2)_{V_2} = (C_1)_{f_1}^{n_2/n_1} (V_2)^{-n_2/n_1} f_1 \quad (3.9)$$

All the quantities on the R.H.S being known, $(C_2)_{V_2}$ is obtained. A second value of $(C_2)_{V_2}$ is got by considering the tool-life, T_{22} corresponding to speed V_2

from the second multispeed test, i.e., at feed f_2 . From the two equations for T_{22} similar to equations (3.7), (3.9), one obtains

$$(C_2)_{V_2} = (C_1)_{f_2}^{n_2/n_1} (V_2)^{-n_2/n_1} f_2 \quad (3.10)$$

The mean value of $(C_2)_{V_2}$, from Equations (3.9) and (3.10), may be quoted.

In the above determination of the feed parameters n_2 , C_2 , of Equation (2.5) from two multispeed tests, each conducted with a different feed, the basic assumption is the constancy of n_1 and n_2 , i.e. the separability of speed and feed effects. This, as mentioned earlier, is inherent in the very nature of a tool-life equation of the form of Equation (3.1). In practice, in conducting two multispeed tests, one would obtain different values of n_1 , due to the experimental randomness of tool-life data. The average n_1 value would then have to be considered as valid for both tests and the C_1 values for the two tests recomputed accordingly to yield the values of $(C_1)_{f_1}$, $(C_1)_{f_2}$ to be used in Equations (3.6), (3.9) and (3.10).

3.3: Deduction Of Flank and Crater Wear From Total Wear Volume Measurements

In tool-life tests with a single radioactive tool, the chips contain tool-wear particles from both the rake and clearance faces. Earlier methods of separating flank and

crater wear in such tests have already been discussed (Sec. 2.3.2), the Hake - Opitz method being the one most commonly applied. This section outlines a novel approach to the separation of flank and crater wear in tests with radioactive tools.

3.3.1: Assumptions made

The total volumetric wear, W is the most directly measurable quantity in tests with radioactive tools and may be written as,

$$W = W_f + W_c \quad (3.11)$$

where W_f , W_c are respectively the flank and crater wear volumes (assuming random effects, such as the generation of a notch at the outer diameter of the workpiece, to be absent). W_f , W_c may be expressed in terms of the geometry of the wear zones. Thus according to Uehara [13],

$$W = \frac{1}{2} (l_w^2 b' \tan Cl) + \frac{2}{3} (u l_c d') \quad (3.12)$$

where the nomenclature is explained in Fig. 3.3.

Several experimental workers have reported that in Region 2 of the wear-growth curves (Figs. 3.1, 3.2), the wear rate is nearly constant when considering wear-land width, l_w , or crater volume, W_c , as the wear criterion. This is clearly evident, for example, in the results quoted by Chawla and Bhattacharya [19], which show that,

in their experiments the inverse wear-rate for l_w and W_c acquired steady values after the initial stage of high wear rate.

In the proposed method, the basic assumption made follows from the above observations. This is, that, l_w and W_c increase linearly with cutting time, t , i.e.

$$l_w \propto t \quad \text{and} \quad W_c \propto t \quad (3.13)$$

Since $W_f \propto l_w^2$ from Equation (3.12), one may write using Equation (3.13),

$$W_f = a t^2 \quad (3.14 \text{ A})$$

and

$$W_c = b t \quad (3.14 \text{ B})$$

where a and b are constants. Thus the total volumetric wear is assumed to be, from Equation (3.11), of the type

$$W = a t^2 + b t \quad (3.15)$$

where a and b are constants characterising flank and crater wear, respectively.

As discussed in Section 3.1, the initial stage of the wear growth curve is non-linear, and it is only in Region 2 that one may assume l_w and W_c to increase linearly with time. The initial non-linearity due to flank and crater effects is introduced separately into the total volumetric wear, but no attempt is being presently made to model this non-linear behaviour.

The assumption that Equation (3.15) is valid right from $t = 0$ would obviously result in some error in computed tool-life values. This may be illustrated by considering the tool life corresponding to total wear volume itself. Thus, in Fig. 3.4 which considers a typical W - vs - t plot, it is only those points beyond the initial "non-linear" region for which a parabolic fit might be attempted. Such a fit would be of the type $W = at^2 + bt + c$, where c is a positive constant. With the presently modelled flank and crater behaviour, linearity of l_w and W_c is assumed from $t = 0$, the assumed curve, $W = at^2 + bt$, passing through the origin. For a given failure criterion for W , it is clear from Fig. 3.4, that the tool life value, T_{lin} , for the assumed W - behaviour would be different from the actual value, T_{act} . However, the difference would be small if the failure criterion is sufficiently far removed from the region with the non-linear effects.

The effects on the tool-life corresponding to l_w , or W_c , criteria may be illustrated by considering the inverse wear-rate plot for one of these, say W_c . Thus, in Fig. 3.5, the "plateau" region is that corresponding to linear growth of W_c . The constant value of the inverse wear-rate in this region is given by, from Equation 3.14 B,

$$\frac{dt}{dW_c} = \frac{1}{(dW_c/dt)} = \frac{1}{b} \quad (3.16)$$

By assuming linear behaviour of W_c right from $t = 0$, one obtains the tool-life T_{lin} , as the area under the line $\frac{dt}{dW_c} = \frac{1}{b}$. This is clearly greater than T_{act} , as indicated in Fig. 3.5. (For the inverse-wear rate plot for l_w , the constant value of $\frac{dt}{d l_w}$ may be used to deduce a , since using Eq. (3.12), $\frac{dt}{d l_w} = \frac{1}{\infty}$ where $\infty = \left(\frac{2a}{b^2 \tan Cl} \right)^{1/2}$).

3.3.2: Determination of a and b

With Equation (3.15) assumed valid, the deduction of a, b from total volumetric wear measurements is possible in several ways. For a single speed/feed test, one obtains a total wear volume growth curve of the type shown in Fig. 3.4(a). By choosing only points well away from the region having non-linear effects for l_w, W_c , one may carry out a least-squares fit of these points to the expression $W = at^2 + bt + c$. Ignoring c , one obtains the a, b values appropriate to Equation (3.15).

A second approach is to consider the total volumetric wear rate, which from Equation (3.15) is

$$\frac{dW}{dt} = 2 a t + b \quad (3.17)$$

The plot of $\frac{dW}{dt}$ - vs - t would thus be a straight line in the region where non-linear effects of l_w, W_c are absent. a would be obtained from the slope of this straight line and b would be the intercept.

It can be seen that neither of the above two methods may be applied to a radioactive test of the multi-feed or multispeed type, since such tests do not provide explicit information about the variation of the total wear volume, W , with t . What is, in fact, obtained is the variation of (for several speeds, or feeds, as the case may be), wear rate with cumulative wear. With Equation (3.15) assumed valid, consider the square of the total volumetric wear rate. From Equation (3.17),

$$\begin{aligned} \left(\frac{dW}{dt} \right)^2 &= (2at + b)^2 = 4a^2t^2 + 4abt + b^2 \\ &= 4a(at^2 + bt) + b^2 \end{aligned} \quad (3.18)$$

or using Equation (3.15)

$$\left(\frac{dW}{dt} \right)^2 = 4aW + b^2 \quad (3.19)$$

Equation (3.19) is a useful result for applying to multi-feed, multispeed total volumetric wear data, in that the plot of $\left(\frac{dW}{dt} \right)^2$ - vs - W would be a straight line with 'a' obtainable from the slope and b from the intercept. It may be noted, however, that the effect of initial nonlinearities in l_w , W_c have to be ignored in the very deduction of a , b from Equation (3.19). This follows from the fact that, in practice, one would be considering, on the R.H.S. of Equation (3.19), the actual cumulative W obtained in a particular test. It may be easily verified that this slightly affects the deduced b value (i.e. intercept of the straight line) but not a , (the slope).

Once a and b have been determined (for a certain feed, speed), Equations (3.14 A), (3.14 B) may be used to obtain the tool life corresponding to a given l_w , of W_c , failure criterion. Such tool-life values, as already discussed, would correspond to T_{lin} and differ slightly from T_{act} (Sec. 3.3.1). Equation (3.15) gives the tool life corresponding to a failure criterion W .

CHAPTER IV

EXPERIMENTAL PARTICULARS

4.1: Cutting Tools and Work Material

The experimental work was carried out using Miranda Super-Treble Swastik H.S.S. tool bits, weighing ~ 10 gm each and containing 10% Cobalt. The tool bits had been irradiated about a year prior to the commencement of the present experiments, in a thermal neutron flux of 7.5×10^{12} n/cm²-sec for 24 hrs. The specific activity, almost entirely due to ⁶⁰Co, was of the order of 3 m Ci/gm. Each bit had been ground at both ends to the following geometry:

Back rake angle	0°	Side rake angle	15°
Side relief angle	5°	End relief angle	5°
End cutting-edge angle	10°	Side cutting-edge angle	0°
Nose radius	0		

In order to minimise ambiguities in the interpretation of results, orthogonal cutting condition (using tubes) were employed in all the experiments. The basic work material presently used was obtained in the form of seamless mild steel ($\sim 0.15\%$ carbon) tubes of I.D. 57 mm, O.D. 70 mm and of average hardness 190 HB. Specimen prepared for the machining tests were of ~ 1.4 mm wall thickness, 65 mm mean diameter and typically 40 cm bore length.

4.2: The Lathe and Counting Set-ups

A 10 HP HMT Lathe was used for the present experiments. An additional tool post was mounted on guide ways provided on the carriage to enable the application of the Hake-Opitz method for flank, crater wear separation. Radiation levels with the radioactive tool in position, were maintained well below maximum permissible levels by using appropriate lead shielding as indicated in Fig. 4.1. A general view of the lathe set-up is shown in Plate 1.

In the course of the experiments, considerable time was spent in starting and stopping the lathe and in changing the feed or speed during multifeed/multispeed tests. Suitable extension rods were designed for the lathe controls so as to minimise the radiation exposure during these operations.

For independent movement of the front and rear tool, the compound slide was rotated through 90° . The movement of the rear tool was obtained on the cross-slide, and the front tool movement was achieved through the compound slide. Plate 1 shows this arrangement. The special type tool posts available on this production lathe were advantageous in centering. To enable easy positioning and viewing of the radioactive tool, an adjustable mirror stand was fabricated and mounted on the rear side of the lathe.

A special drawer-type, chip collection box was prepared for easy removal of the radioactive chips. One metre tongs were used for removing the drawers containing the chips, the latter being packed in numbered, tin pill-boxes of 36 mm diameter, 18 mm height.

A block diagram of the counting set-up used for γ -counting the chip samples and standard sources is shown in Fig. 4.2. The Na I crystals were of 50 mm x 50 mm size. A sample changer was used with the two detectors mounted vertically above and below, about 5 cms apart. A 10 cm thick lead shield around each detector ensured adequate background discrimination.

4.3: Experimental Procedures

4.3.1 Deduction of absolute wear volumes

γ - counting of the pill-box chip samples was carried out with each detector channel set on both ^{60}Co photopeaks. The sum of the two single-channel, background-corrected counts, over a period of 500 seconds, was taken as the relative measure of volumetric wear. A standard ^{60}Co point source was used to check for possible electronic drifts during the counting of the chip samples. Statistical accuracies presently obtained in the counting of individual chip samples were $\pm 8\%$ for both flank and crater.

In order to make the results absolute, the activity of one of the more active pill box samples, S_c , was normalised to the activity of a standard ^{60}Co point-source (Standard A) by γ - γ coincidence counting [6]. Standard A was, in turn, known to represent a certain volume of irradiated tool material, the normalisation against small reference pieces of tool material having been earlier carried out by single γ counting. The absolute wear volume in Chip Sample S_c being known, the count-rates of all other chip samples, counted under identical conditions, could be normalised to yield absolute results.

4.3.2: Multifeed tests

For obtaining $\frac{dt}{dw}$ - v s - w curves, for a given cutting speed (V) but several different feeds, the test was started off with the lowest feed, f_1 . Three sets of chip samples were collected, over typically 15 sec. machining intervals, from the front and back tools. The feed was changed to the next higher value, f_2 , and three further sets of chip samples obtained. This was then done for feed f_3 . The feed was then changed back to f_1 and the procedure outlined above was repeated.

As in the case of multispeed testing [19], counting of any given sample would yield a wear-rate, with a corresponding value of cumulative wear. In the present

case, points would sequentially be generated on the $\frac{dt}{dw} - v_s - w$ curves for f_1, f_2, f_3 , the first three chip samples giving three points on the f_1 curve, the next three giving points on the f_2 curve, and so on. In effect, there would be simultaneous generation of the inverse wear-rate curves for the three feeds, and thus of three (f_i, T_i) pairs corresponding to a given failure criterion.

In determining tool-life parameters from multi-feed tests, three different criteria have been presently considered viz., for wear-land width, crater wear volume and total wear volume (Sec. 2.1).

4.3.3: Extension of multispeed testing

The deduction of feed parameters, n_2 and C_2 from a pair of multispeed tests (Sec. 3.2) was achieved by conducting two multispeed tests with two different constant-feed values which spanned the feed range used for the multifeed tests (Sec. 3.2). The speed range for the two multispeed tests was identical, viz. $V_1 - V_3$, where $V_1 < V_2 < V_3$, V_2 being the constant speed employed in the multifeed tests.

4.3.4: Conventional tests

Conventional orthogonal tests to determine n_2 and C_2 (with l_w criterion) were conducted with the same

mild steel tube material and with unirradiated H.S.S. tool bits of identical specifications. A plot of l_w - vs - t was separately obtained for each feed value by microscopical examination of the tool clearance face at intervals of typically 5 minutes cutting time.

4.3.5: Validation of the proposed method for flank, crater separation

A single speed/feed test was carried out at the intermediate speed (V_2) of the multispeed test range and the intermediate feed of the multifeed test range, in order to validate the approach outlined in Sec. 3.3 for separating flank and crater effects. The points to be confirmed were

- i) the linear growth of l_w and W_c after the initial non-linear stage,
- ii) consistency in a , b values deduced from wear volume results (Sec. 3.3.2) using, separately, Equations (3.15), (3.17) and (3.19), and
- iii) the comparison of a , b values deduced in (ii) with actual values (Sec. 3.3.1) obtained from Hake-Opitz separation (c.g. from Equation (3.16) for b).

A multifeed test was conducted without Hake-Opitz separation i.e. without using a rear tool, to further

test the validity of the present method. This test was carried out with a test specimen of bore length > 50 cms., so that the region of linear l_w , W_c growth might be expected to be better defined than in the other tests. Total volumetric wear rate data from this region was analysed and a , b values deduced from Equation (3.19) to yield comparisons with results from the other experiments.

Attempts were also made to analyse the multifeed, multispeed data for total volumetric wear from the earlier experiments to deduce appropriate a , b values using Equation (3.19).

CHAPTER V

RESULTS AND DISCUSSIONS

5.1: Multifeed Tests

As a check on the repeatability of results, two separate multifeed tests, MF1 and MF2, were carried out under almost identical cutting conditions (Table 5.1).

Table 5.1

Cutting Conditions For Multifeed Tests

Test No	MF1	MF2
Cutting Speed (m/min)	22.8	23.0
Effective Feed (mm/rev)	0.081, 0.125, 0.168	0.079, 0.117, 0.159
Average Tube Thickness (mm)	1.40	1.42

Figs. 5.1 - 5.3 show the results obtained in Multifeed Test 1. Fig. 5.1 is the plot of inverse wear land growth rate, against cumulative wear land ($\propto \sqrt{W_f}$, Equation (3.12)). Similarly, the inverse crater volume growth rate is shown plotted against cumulative crater volume (W_c) in Fig. 5.2, and the inverse total wear volume growth rate ($\frac{dt}{dW}$) against cumulative total wear volume (W) in Fig. 5.3.

Figs. 5.4 - 5.6 are the corresponding plots obtained in Multifeed Test 2.

5.1.1 Tool-life values obtained from Multifeed Tests:

As discussed in Sec. 3.1, the tool-life values for the three feeds used in a particular test were obtained from the areas under the corresponding curves unto the criterion chosen.

The criteria used in the present analyses were,

Wear land width, $l_w = 0.4 \text{ mm}$

Crater volume, $W_c = 12 \text{ ucc}$

Total wear volume $W = 20 \text{ ucc}$

Table 5.2 summarises the tool-life values obtained with the above criteria.

Table 5.2

Tool-life Values (in minutes) From Multifeed Tests

Criterion	f_1	MF1	MF2
Wear land $l_w = 0.4 \text{ mm}$	f_1	$T_1 = 22.5$	$T_1 = 23.1$
	f_2	$T_2 = 10.3$	$T_2 = 10.6$
	f_3	$T_3 = 7.6$	$T_3 = 7.7$
Crater volume 12 ucc	f_1	$T_1 = 20.8$	$T_1 = 20.9$
	f_2	$T_2 = 12.1$	$T_2 = 12.3$
	f_3	$T_3 = 6.4$	$T_3 = 6.5$
Total wear volume 20 ucc	f_1	$T_1 = 18.8$	$T_1 = 20.1$
	f_2	$T_2 = 9.0$	$T_2 = 9.7$
	f_3	$T_3 = 6.6$	$T_3 = 6.8$

5.1.2: Feed parameters from Multifeed Tests

Using the (f_i, T_i) pairs from Table 5.2, n_2 and C_2 values for the Taylor-type equation, Equation (2.5), were obtained. Table 5.3 summarises the results, which are seen to be quite consistent.

Table 5.3
Average n_2 , C_2 values from Multifeed Tests

Criterion		MF1		MF2	
		n_2	C_2	n_2	C_2
Wear land	= 0.4 mm	0.76	0.79	0.73	0.72
Crater volume	= 12 ucc	0.63	0.57	0.61	0.51
Total wear volume	= 20 ucc	0.77	0.74	0.70	0.62

5.2: Multispeed Tests

As mentioned in Sec. 4.4.3, two multispeed tests (MS1 and MS2) using different constant feed values were conducted for validating the alternative approach for studying feed effects (Sec. 3.2). Cutting conditions for these two tests are given in Table 5.4.

Table 5.4

Cutting Conditions for Multispeed Tests

Test	MS1	MS2
Effective feed (mm/rev)	0.178	0.080
Cutting speeds (m/min)	17.8, 22.6, 28.2	18.0, 22.8, 28.8
Average tube thickness (mm)	1.39	1.41

Referring to Tables 5.1 and 5.4 it is seen that the intermediate speed, V_2 (~ 22.8 m/min), for the multispeed tests corresponds to the constant speed used in the multi-feed tests, while the constant feed values in the two multispeed tests (0.178 mm/rev for MS1 and 0.080 mm/rev for MS2) span the feed range for the multifed tests. This was, of course, done so as to be consistent with the assumption that n_1 , n_2 are constants over the speed, feed ranges being considered.

Results for MS1 are shown in Figs. 5.7 - 5.9.

Fig. 5.7 is the plot of $\frac{dt}{d l_w}$ - vs - l_w . In Fig. 5.8 $\frac{dt}{d W_c}$ is plotted against W_c and Fig. 5.9 shows the plot of $\frac{dt}{d W}$ - vs - W .

Figs. 5.10 - 5.12 show the corresponding plots in MS2.

5.2.1: Tool-life values obtained from MS1 and MS2

Table 5.5 shows the tool-life values obtained from MS1 and MS2 using the l_w , W_c and W criteria given in Sec. 5.1.1.

Table 5.5

Tool-life values (in minutes) from Multispeed Tests

Criterion	V_i	NS1	MS2
Wear-land $l_w = 0.4 \text{ mm}$	V_1	$T_1 = 11.7$	$T_1 = 29.0$
	V_2	$T_2 = 7.0$	$T_2 = 15.1$
	V_3	$T_3 = 4.5$	$T_3 = 11.6$
Crater volume $= 12 \text{ } \mu\text{cc}$	V_1	$T_1 = 10.4$	$T_1 = 27.5$
	V_2	$T_2 = 6.0$	$T_2 = 18.5$
	V_3	$T_3 = 2.7$	$T_3 = 11.0$
Total wear volume $= 20 \text{ } \mu\text{cc}$	V_1	$T_1 = 9.9$	$T_2 = 25.4$
	V_2	$T_2 = 6.1$	$T_2 = 15.3$
	V_3	$T_3 = 3.0$	$T_3 = 6.7$

Making use of the (V_i, T_i) pairs obtained in the multispeed tests the constants n_1, C_1 of Taylor's equation (Equation (2.1)) were deduced in each case. Table 5.6 gives the separate values obtained for the two tests.

Table 5.6

Average n_1, C_1 values from Multispeed Tests

Test	MS1		MS2	
	n_1	C_1	n_1	C_1
$l_w = 0.4 \text{ mm}$	0.48	59	0.63	137
$W_c = 12 \text{ } \mu\text{cc}$	0.35	43	0.54	106
$W = 20 \text{ } \mu\text{cc}$	0.40	45	0.37	60

5.2.2: Feed parameters from the Multispeed Tests

For calculation of the feed exponent n_2 and the constant C_2 (Equation 2.5) from the multispeed-test data, n_1 and n_2 are assumed to be independent constants (Sec. 3.2) over the speed, feed ranges under consideration. Accordingly, the variation in the n_1 results for MS1, MS2 (Table 5.6) have to be attributed to random effects, and an average n_1 value should be considered for computing appropriate $(C_1)_{f_1}$, $(C_1)_{f_2}$ values for the two tests. Equations (3.6), (3.9) and (3.10) may then be applied for the deduction of n_2 and $(C_2)_{V_2}$. Table 5.7 summarises the results of such an analysis.

Table 5.7

Average n_2 and C_2 values from Multispeed Tests

Criterion	n_1	$(C_1)_{f_1}$	$(C_1)_{f_2}$	n_2	$(C_2)_{V_2} (i)$	$(C_2)_{V_2} (ii)$
$l_w = 0.4$ mm	0.56	67	111	0.87	0.95	0.93
$W_c = 12$ μ cc	0.45	49	82	0.70	0.62	0.62
$W = 20$ μ cc	0.39	44	63	0.86	0.78	0.77

It may be noted that two values of the feed constant $(C_2)_{V_2}$ are obtained, depending upon which of Equations (3.9), (3.10) is applied. The average result may be quoted.

5.3: Conventional Tests

Conventional orthogonal-cutting tests were conducted to obtain n_2 , C_2 values (for l_w - criterion) which could be compared with the radioactive-tool testing results. Table 5.8 gives the cutting conditions for three conventional tests used for generating three (f_i, T_i) pairs with $V_2 \sim 23.0$ m/min.

Table 5.8

Cutting conditions for conventional tests

Test No.	0	1	0	2	0	3
Feed (mm./rev.)		0.081		0.125		0.168
Cutting speed (m/min.)		23.1		23.0		22.9
Average tube thickness (mm.)		1.42		1.45		1.44

Fig. 5.13 shows the plot of wear-land growth against cutting time. Tool-life values were extrapolated from the curves for the chosen criterion of $l_w = 0.4$ mm. The n_2 , C_2 values obtained from these (f_i, T_i) pairs are given in Sec. 5.4.

It should be mentioned that a second conventional check on the validity of the nuclear techniques was the microscopical observations of the cumulative l_w for the various tests with radioactive tools. This was done using

a shielded tool-maker's microscope with an extension for the eyepiece to minimise the radiation exposure [21]. Satisfactory agreement was obtained with cumulative l_w values deduced from the nuclear tests.

5.4: Comparison Of n_2 , C_2 Results From Multifeed, Multispeed and Conventional Tests

Table 5.9 gives this comparison.

Table 5.9

Comparison of n_2 , C_2 values obtained from MF, MS and Conventional tests

Criterion	MF		MS		Conventional	
	n_2	C_2	n_2	C_2	n_2	C_2
$l_w = 0.4 \text{ mm}$	0.75	0.76	0.87	0.94	0.72	0.99
$W_c = 12 \text{ } \mu\text{cc}$	0.62	0.54	0.70	0.62	-	-
$W = 20 \text{ } \mu\text{cc}$	0.74	0.68	0.86	0.78	-	-

The n_2 , C_2 values obtained are seen to be in reasonable agreement, considering (a) systematic differences in the initial portions of the crater curves for the multi-feed and multispeed tests and (b) the scatter in the experimental data. Separate tests were conducted to investigate the crater behaviour, but no conclusions could be drawn except ^{that} the effect was random.

5.5: Deduction of Flank and Crater Wear Volumes From Total Wear Volume Measurements

5.5.1: Single speed/feed test

A single speed/feed test was carried out with the cutting conditions given in Table 5.10.

Table 5.10

Cutting conditions for single speed/feed test

Effective feed (mm/rev)	= 0.094
Cutting speed (m/min.)	= 22.60
Average tube thickness mm	= 1.40

Fig. 5.14 shows the wear growth curves obtained. It is seen that the crater volume and the wear-land width do exhibit linearity after initial non-linear behaviour, with the total wear volume growth curve being of the type $W = at^2 + bt + c$. Figs. 5.15 - 5.17 show the plots of $\frac{dt}{dl_w}$ - vs - l_w , $\frac{dt}{dW_c}$ - vs - W_c and $\frac{dt}{dW}$ - vs - W , respectively. The actual values of the constants a and b were read off from Figs. 5.15 and 5.16 respectively (Sec. 3.3.1).

Figs. 5.18 (a) and (b) show the $\frac{dW}{dt}$ - vs - t and $(\frac{dW}{dt})^2$ - vs - W plots obtained for this single speed/feed test. The intercept and the slope of the straight lines gave a and b values (Sec. 3.3.2). In Table 5.11 these deduced values are compared with the actual a , b values, as

well as with values obtained from a least squares fit of W in the "linear" region to the expression $W = at^2 + bt + c$.

Table 5.11

Comparison of deduced and actual a, b values, in SSF.

Actual Values	Deduced Values		
	dW/dt -vs- t plot	$(dW/dt)^2$ -vs- W plot	$W = at^2 + bt + c$ plot
$a = 0.026$	$a = 0.039$	$a = 0.026$	$a = 0.030$
$b = 0.50$	$b = 0.55$	$b = 0.64$	$b = 0.55$
-	-	-	$c = 0.15 \text{ ucc}$

(Units: $a - \text{ucc}/\text{min}^2$, $b - \text{ucc}/\text{min}$).

Errors in the above deductions of a, b were considerable in the present case due to the large scatter in the experimental points (Figs. 5.15 - 5.17). It will be seen later (Sec. 5.5.4) that, if the plots of $(\frac{dW}{dt})$ -vs- t and $(\frac{dW}{dt})^2$ -vs- W are well defined much more reliable a, b values can be deduced. Table 5.12 compares the tool-life values obtained using the a, b values obtained from Table 5.11 in Equations 3.14(A), (B) and Ecn.(3.15), with the actual (non-linear effects included) tool-life values from the single speed/feed test.

Table 5.12

Comparison of Tool-life values (in mins) from a,b values
with the Actual Tool Life in SSF.

Criterion	Using actual a,b values	Using deduced a,b values			Actual Tool Li from SS
		$\frac{dW}{dt}$ -vs-t plot	$(\frac{dW}{dt})^2$ -vs-W plot	$W = at^2+bt+c$ plot	
$l_w = 0.4$ min	19.4	15.9	19.4	18.0	17.3
$W_c = 12$ μ cc	24.0	21.8	18.8	18.2	23.2
$W = 20$ μ cc	19.7	16.7	18.0	17.0	17.0

5.5.2: Multifeed Test 3

This test was performed without using the Hake and Opitz method for the separation of flank and crater. The cutting conditions are tabulated in Table 5.13.

Table 5.13

Cutting conditions for Multifeed test 3.

1)	Effective feed (min/rev.):	0.081, 0.125, 0.168
2)	Cutting speed (m/min):	23.10
3)	Average tube thickness (mm):	1.43

Fig. 5.19 shows the plots obtained for $(\frac{dW}{dt})^2$ -vs-W. The slope and the intercept of the straight line portions of the three curves gave a,b values corresponding to the three feeds used. As this test was performed with a single tool it was not possible to check the deduced a,b values with actual ones, the only inverse wear-rate curve obtained being $\frac{dt}{dW}$ -vs-W (Fig. 5.20). However, for making a comparison, the results of Multifeed Test 1, (Figs. 5.1 and 5.2) were made use of because the cutting conditions for MF1, MF3 were similar. Table 5.14 gives this comparison.

Table 5.14

Comparison of deduced a,b values in MF3 with actual a,b values of MF1.

Feed	Deduced values for MF3		Actual values from MF1	
	a(ucc/min ²)	b(ucc/min)	a(ucc/min ²)	b(ucc/min)
f ₁	0.014	0.46	0.013	0.45
f ₂	0.036	1.08	0.052	0.79
f ₃	0.082	1.61	0.105	1.55

Tool-life values for l_w , W_c and W criteria were calculated by using the a,b values of Table 5.14. These values are compared with the actual tool-life results from MF1 (Sec. 5.1.1) in Table 5.15. It should be noted that the actual tool-life values corresponding to total wear volume criterion

were obtained by considering the $(\frac{dt}{dW})$ -vs- W plot of MF3, i.e. Fig. 5.20, whereas for l_w and W_c criteria, results of MF1 were made use of.

Table 5.15

Comparison of Tool-life values (in mins), from a,b values in MF3 with Actual Tool-life values from MF1 and MF3.

Criterion	Using deduced a,b values (MF3)			Using actual a,b values (MF1)			Actual Tool-life
							From MF1
$l_w = 0.4 \text{ mm}$	f_1	T_1	= 26.7	T_1	= 27.5		$T_1 = 22.5$
	f_2	T_2	= 16.7	T_2	= 13.7		$T_2 = 10.3$
	f_3	T_3	= 11.0	T_3	= 9.7		$T_3 = 7.6$
$W_c = 12 \text{ ucc}$	f_1	T_1	= 26.0	T_1	= 27.2		$T_1 = 20.8$
	f_2	T_2	= 11.1	T_2	= 15.4		$T_2 = 12.1$
	f_3	T_3	= 7.5	T_3	= 7.8		$T_3 = 6.4$
$W = 20 \text{ ucc}$	f_1	T_1	= 24.8	T_1	= 25.8		$T_1 = 21.6$
	f_2	T_2	= 12.9	T_2	= 13.5		$T_2 = 10.0$
	f_3	T_3	= 8.6	T_3	= 8.3		$T_3 = 6.6$

It should be mentioned that errors in the fitting of the f_2 -data in MF3 were considerable due to random variations of wear rate between successive sets of points for this feed (Fig. 5.19).

5.5.3: Multifeed Test 2

The proposed method was applied to this test wherein Hake - Opitz method of separation had been used. The actual a, b values from Figs. 5.4 and 5.5 were compared with a, b values deduced by the proposed technique. Fig. 5.21 shows the plots obtained for $(\frac{dW}{dt})^2$ -vs- W . It should be noted that the constant wear-rate region of the inverse wear-rate curves (Figs. 5.4 and 5.5) reached a constant value after about three sets of points. Only two sets were therefore available in the "linear" region. The experimental data was thus insufficient to deduce reliable a, b values, as is evident from the inconsistency indicated in Table 5.16.

Table 5.16

Comparison of deduced and actual a, b values in MF2.

Feed	Deduced		Actual	
	$a(\mu\text{cc}/\text{min}^2)$	$b(\mu\text{cc}/\text{min})$	$a(\mu\text{cc}/\text{min}^2)$	$b(\mu\text{cc}/\text{min})$
f_1	0.013	0.41	0.012	0.46
f_2	0.027	1.20	0.049	0.80
f_3	0.055	2.00	0.099	1.59

5.5.4: Other Tests

The multispeed tests carried out in the present work showed considerable scatter when the data obtained was plotted as

$(\frac{dW}{dt})^2$ -vs- W . It was for this reason that one of the multispeed tests reported recently by Bhattacharya [21] was re-analysed by applying the presently proposed technique for separation of flank and crater wear. To avoid any ambiguity, this test (Multispeed test 2 in Bhattacharya's work) is here called OT1 (Other Test 1).

The nature of the inverse flank and crater wear rate plots in OT1 is indicated in Fig. 5.22, and is seen to be of the same type as obtained in the present experiments. The scatter in the data points was, however, much less. The $(\frac{dW}{dt})^2$ -vs- W plot for OT1 is shown in Fig. 5.23. a, b values deduced by the present method are compared with the actual a, b values in Table 5.17.

Table 5.17

Comparison of deduced and actual a, b values in OT1.

Speed (m/min)	Deduced		Actual	
	$a(ucc/min^2)$	$b(ucc/min)$	$a(ucc/min^2)$	$b(ucc/min)$
$V_1 = 22.5$	0.008	0.65	0.009	0.61
$V_2 = 33.2$	0.015	0.85	0.015	0.83
$V_3 = 55.3$	0.043	1.31	0.047	1.36

The tool-life values obtained by using the above a, b values in Eqns. 3.14(A) and (E) and (3.15) are compared as before with the actual tool-life values in Table 5.18. It is seen that the proposed method gives reliable results if the $(\frac{dV}{dt})^2$ -vs- W plot, or for that matter, the inverse wear-rate curves are well defined. (It may be noted from Table 5.18 that the failure criteria used by Phattacharya were slightly different from those employed in the present work).

Table 5.18

Comparison of Tool-life values (in mins) from a, b values with Actual Tool-life values in OT1.

Criterion	Using Actual a, b values	Using Deduced a, b values	Actual Tool- Life*
$l_w = 0.25 \text{ mm}$	$V_1 \quad T_1 = 19.8$	$T_1 = 21.0$	$T_1 = 17.6$
	$V_2 \quad T_2 = 15.3$	$T_2 = 15.3$	$T_2 = 12.4$
	$V_3 \quad T_3 = 8.8$	$T_3 = 9.4$	$T_3 = 7.3$
$W_c = 10 \text{ ucc}$	$V_1 \quad T_1 = 16.4$	$T_1 = 15.4$	$T_1 = 14.8$
	$V_2 \quad T_2 = 12.0$	$T_2 = 11.8$	$T_2 = 11.2$
	$V_3 \quad T_3 = 7.4$	$T_3 = 7.6$	$T_3 = 7.1$
$W = 12.5 \text{ ucc}$	$V_1 \quad T_1 = 16.5$	$T_1 = 16.1$	$T_1 = 14.7$
	$V_2 \quad T_2 = 12.3$	$T_2 = 12.1$	$T_2 = 10.9$
	$V_3 \quad T_3 = 7.3$	$T_3 = 7.7$	$T_3 = 6.8$

* Data from [21].

A single speed test reported by Bhattacharya (21) was also reanalysed by the present method. This test is referred to as OT2 here. The $(\frac{dW}{dt})$ -vs- t and $(\frac{dW}{dt})^2$ -vs- W plots are shown in Fig. 5.24 and 5.25, respectively. The comparison of deduced and actual a, b values is given in Table 5.19.

Table 5.19

Comparison of Deduced and Actual a, b values in OT2.

Actual	Deduced		
	$\frac{dW}{dt}$ -vs- t plot	$(\frac{dW}{dt})^2$ -vs- W plot	$W = at^2 + bt + c$ plot
$a = 0.015$	$a = 0.013$	$a = 0.014$	$a = 0.013$
$b = 0.86$	$b = 0.88$	$b = 0.87$	$b = 0.93$
-	-	-	$c = 0.78 \text{ } \mu\text{cc}$

(Units: $a - \mu\text{cc}/\text{min}^2$, $b - \mu\text{cc}/\text{min}$).

These a, b values were used, as before, to obtain tool-life values from Equations 3.14(A), 3.14(B) and (3.15). Table 5.20 summarises the results. It is evident that the proposed technique gives reliable results when the experimental data has good statistical accuracy.

Table 5.20

Comparison of Tool-life values (in mins.) from a,b values
with the Actual Tool life values in OT2.

Criterion	Using Actual a,b values	Using Deduced a,b values			Actual tool- life*
		(dW/dt)-vs-t plot	(dW/dt) ² - vs-W plot	$W = at^2+bt+c$ plot	
$l_w=0.25$ mm	15.3	16.5	15.9	16.5	12.4
$W_c=10$ ucc	12.0	11.4	11.5	10.8	11.2
$W=12$ ucc	12.3	12.1	12.0	11.0	10.9

* Data from (21).

CHAPTER VI

CONCLUSIONS AND SCOPE FOR FURTHER WORK

6.1:Conclusions

Radiotracer techniques have been employed for the investigation of feed effects. Feed parameters n_2 , C_2 (Eqn. (2.5)) were deduced by performing multifeed tests as discussed in Secs. 3.1, 4.3.2. Values of these parameters were compared with the values obtained by extending the multispeed testing approach (Secs. 3.2, 4.3.3). It was found that, owing to statistical errors (typically $\pm 8\%$), there was significant scatter in the experimental data. This scatter was reflected in the comparison of n_2 , C_2 values but, nevertheless, reasonable agreement was obtained.

For separating flank and crater components of total volumetric wear, a novel method has been proposed taking advantage of the different characteristic variations of flank and crater wear with cutting time (Secs. 3.3, 4.3.5). Experimental validation of the proposed method was obtained by carrying out a single speed/feed test and comparing deduced flank, crater components of the total wear with actual results from the Hake-Opitz method of separation.

The Hake-Opitz method, though widely used in radioactive tool testing, has certain shortcomings. These are:

- (i) difficulties in the accurate setting of twin tools,
- (ii) uncertainty in the effective feed values obtained, and
- (iii) the need for separate counting of flank, crater chip samples.

All these difficulties are eliminated in the proposed method, wherein a single radioactive tool is employed and a single set of chip samples is obtained for counting.

The proposed method was also applied to a multifeed test using a single tool, and deduced tool-life results for flank and crater wear were compared with results obtained from a similar test employing the Hake-Opitz method. Considering that the experimental data from this multifeed test was limited in extent as well as statistical accuracy, the agreement obtained was reasonable. By reanalysing some earlier conducted experiments (OT1, OT2, Sec. 5.5.4), it was shown that considerably more consistent tool-life values can be deduced when the inverse wear-rate curves are better defined.

6.2: Scope for Further Work:

It has been presently shown that multi-speed tests can be extended to yield feed parameters which are consistent with values from multi-feed tests. A further possible extension of multispeed testing would be the deduction of depth-of-cut effects, assuming Ecn. (2.2) to be valid. Just as two

multispeed tests with different constant-feed values (but same depth of cut, d) have been shown to give n_2 and C_2 , in like manner two multispeed tests with different d -values (but same constant feed) would yield depth of cut parameters. Thus in principle, three multispeed tests could give information on all the three exponents of Eqn. (2.2).

The development of a single wear criterion for tool-life evaluation has been suggested by several workers, e.g. [14]. Total volumetric wear is an obvious choice, particularly in radioactive-tool testing. The arguments against the use of this single criterion, however, are that information on the relative importance of flank and crater effects is not obtained. The presently proposed method for deducing the separate contributions of flank and crater should strengthen the case for the usage of total volumetric wear as a single criterion. A considerable amount of experimental data with different tool/work combination and over a sufficient range of cutting conditions is, however, needed for validating the present approach and for developing the single-criterion concept further.

Considering that orthogonal cutting conditions (i.e. using tubes) were employed throughout the present work it would be meaningful to validate the proposed methods under the more practical conditions of restricted orthogonal cutting.

REFERENCES

1. Merchant, M.E. and Krabachar, E.J., "Radioactive Tracers for Rapid Measurement of Cutting Tool-Life", J. of Appl. Phys., 22, 12 (1951).
2. Merchant, M.E., Ernst, H and Krabacher, E.J., "Radioactive Cutting Tools for Rapid Tool-Life Testing", Trans. A.S.M.E., 75, 549 (1953).
3. Colding, B.N., "Testing of Machinability by Radioactive Methods", Acta Polytechnica Scandinavia, Mel, Stockholm (1958).
4. Wilson, G.F., and McHenry, W.D., "Study of the Radiometric Method and Use of the Liquid Scintillation Technique for Tool-Wear Determination" Trans. A.S.M.E. J. of Engg. for Ind., 87, 47 (1965).
5. Cook, N.H., and Lang, A.B., "Criticism of Radioactive Tool-Life Testing", Trans. A.S.M.E., J. of Engg. for Ind., 85, 381 (1963).
6. Chawla, R., and Bhattacharyya, S.L., "Determination of Absolute Wear by γ - γ Coincidence Counting of Radiotracers", Wear, 43, 175 (1977).
7. Askouri, W.A., et. al., "On line Wear Monitoring by Surface Activation", Int. J. of Appl. Radiation and Isotopes, 26/2, 61 (1975).
8. Cook, N.H., et. al., "Survey of the State of the Art of Tool Wear Sensing Techniques", Survey published by the Materials Processing Laboratory, M.I.T., U.S.A. (1975).
9. Taylor, F.W., "On the Art of Cutting Metals", Trans. A.S.M.E., 28, 31 (1907).
10. Cook, N.H., "Tool-Wear and Tool-Life", Trans. A.S.M.E., J. of Engg. for Ind., 95, 931 (1973).
11. Sen, G.C. and Bhattacharyya, A., "Principles of Metal Cutting", New Central Book Agency, Calcutta, (1969).

12. Trigger, K.J., and Chao, F.T., "An analytical Evaluation of Metal Cutting Temperatures, Trans., A.S.M.E., 73/1, 57 (1951).
13. Colding, R.N., "A Three Dimensional Tool-life Equation and Machining Economics", Trans. A.S.M.E., J. of Engg. for Ind., 81, 239 (1959).
14. Uehara, K., and Takeyama, T., "Characteristics of Tool-Wear based on the volume of Flank and Crater Wear", Ann. C.I.R.P., 24/1, 59 (1975).
15. Wager, J.G., and Barash, M.H., "Study of the Distribution of Life of H.S.S. Tools", Trans. A.S.M.E., J. of Engg. for Ind., 93, 1044 (1971).
16. Solaja, V., "Tool-life Testing by Facing in a Lathe", Wear, 1, 512 (1955).
17. Heggingbotham, W.B., and Pandey, P.C., "Taper Turning Tests Produce Reliable Tool Wear Equations", Proc. 7th Int. M.T.D.R. Conf., Birmingham, 515 (1966).
18. Heggingbotham, W.P., and Pandey, P.C., "A Variable Rate Machining Test for Tool-Life Evaluation" Proc. 8th Int. M.T.D.R. Conf., Manchester, 163 (1967).
19. Chawla, R., and Bhattacharyya, S.L., "Multispeed Tool-Life Tests with Radioactive Tools", To appear in Wear.
20. Taylor, J., "The Tool Wear Time Relationship in Metal Cutting", Int. J. of M.T.D.R., 2, 119 (1962).
21. Bhattacharyya, S.L., "Absolute Tool-Wear and Tool-Life Determination $\gamma - \gamma$ Counting of Radiotracers", M.Tech. Thesis, I.I.T. Kanpur (1976).
22. Chawla, R., "Nuclear Measurements Laboratory", Lecture Notes, I.I.T. Kanpur (1975).

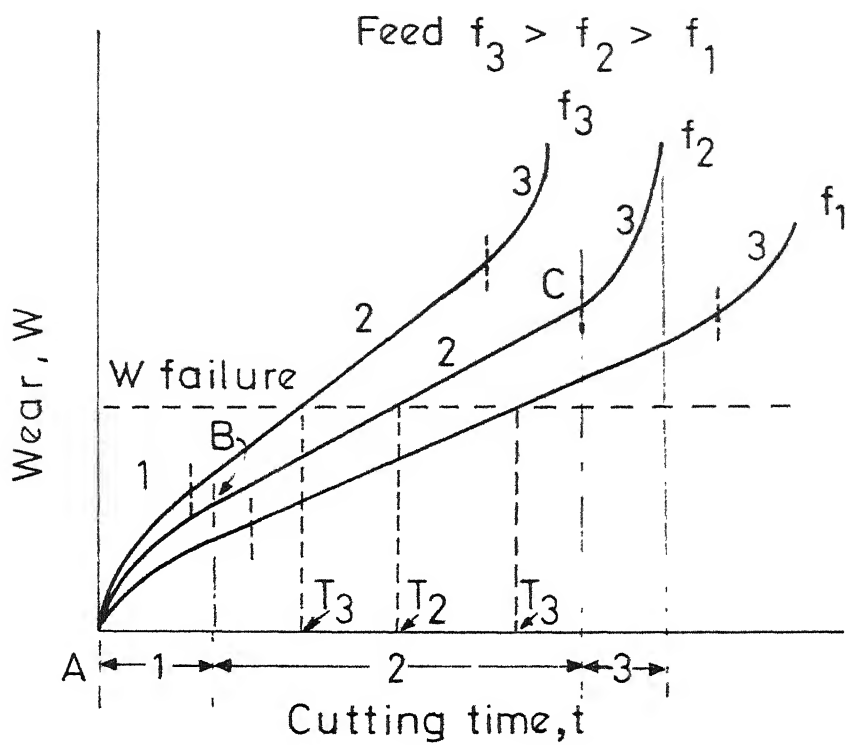


Fig. 3-1 Growth of flank wear-land

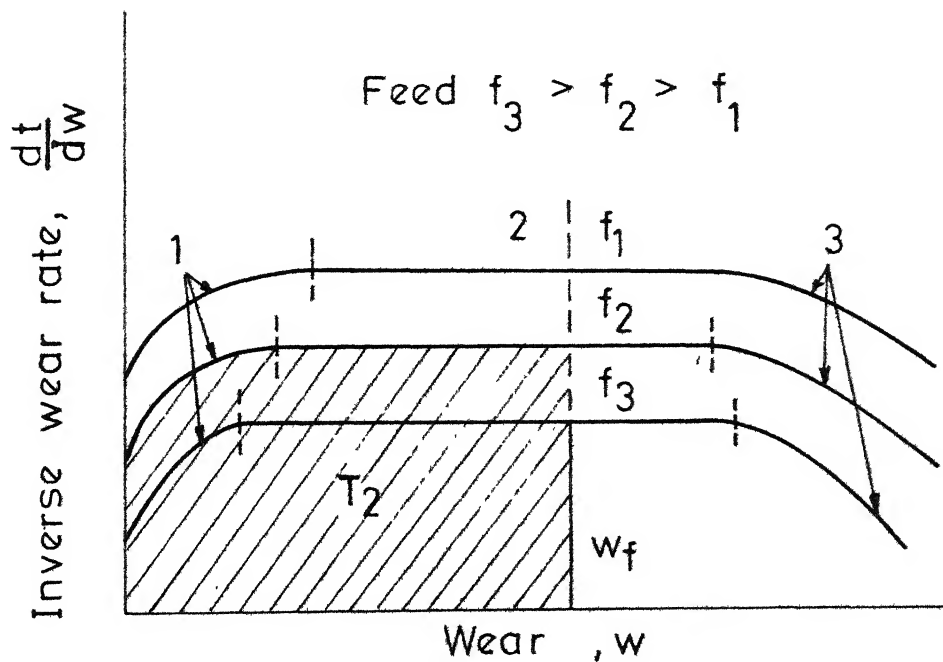


Fig. 3-2 Inverse wear-land growth rate curves

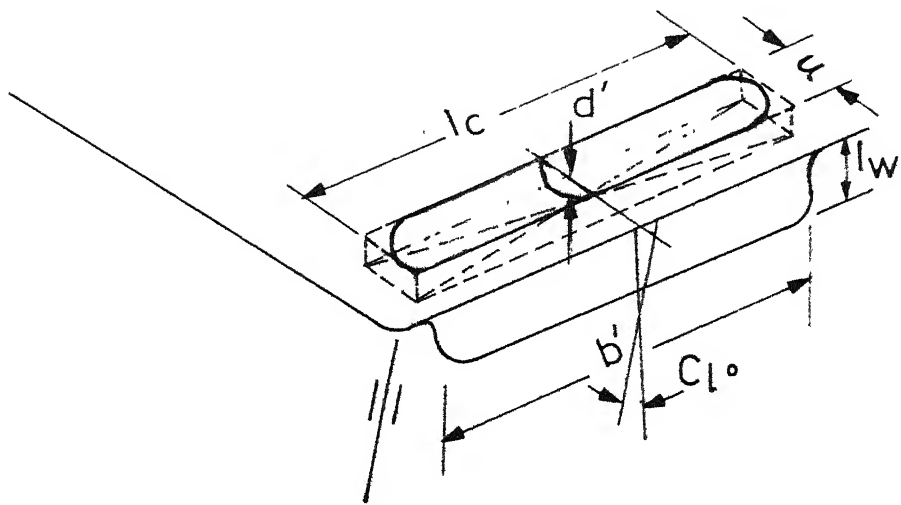


Fig. 3-3 Geometry of tool-wear

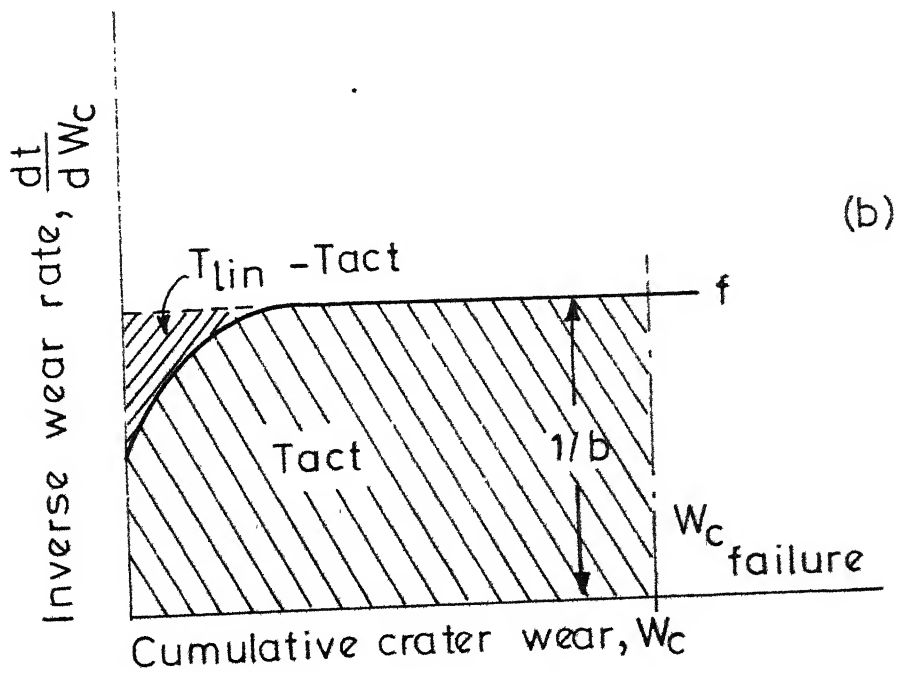
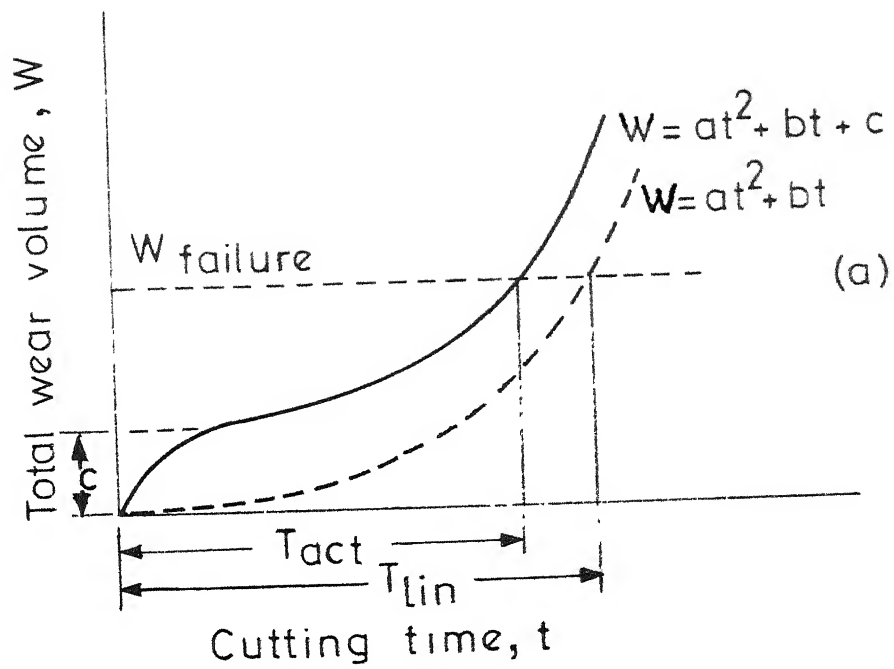


Fig. 3-4 Effect on tool lives with
 (a) Total volume criterion
 (b) Crater volume criterion

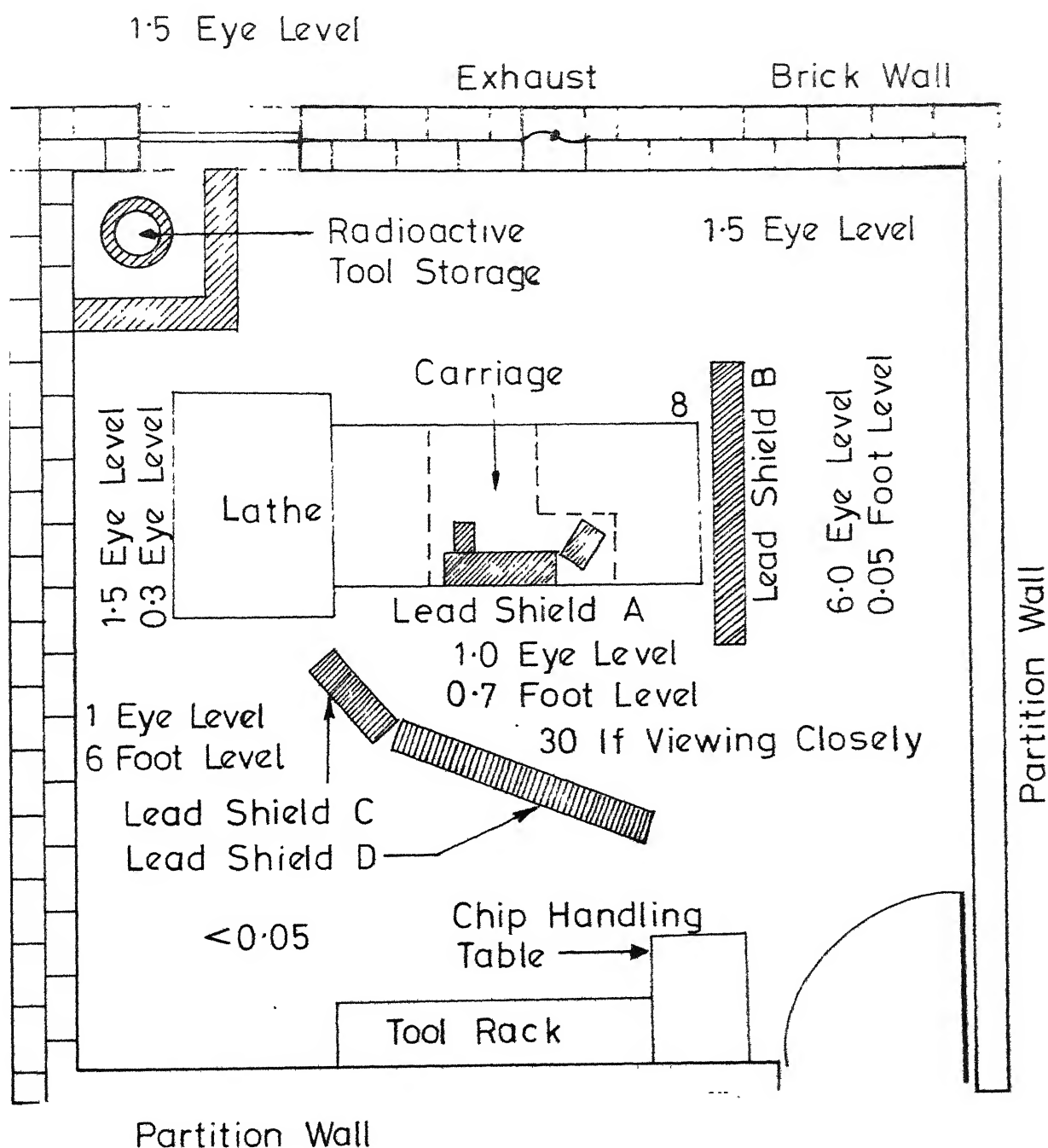


Fig. 4.1 Radiation levels in mR/hr during the machining tests

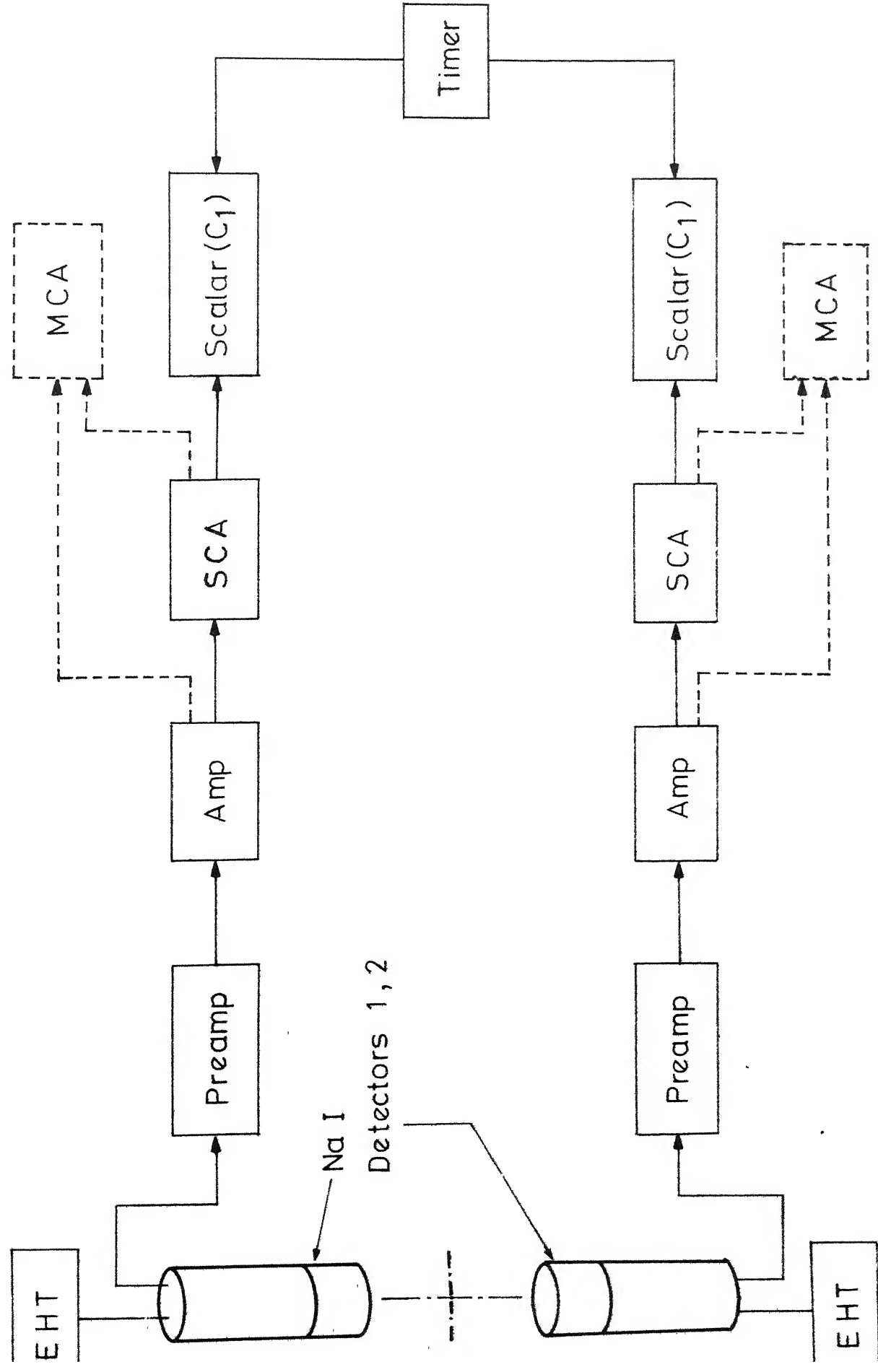


Fig. 4.2 Block diagram of twin Na I scintillation counter set up .

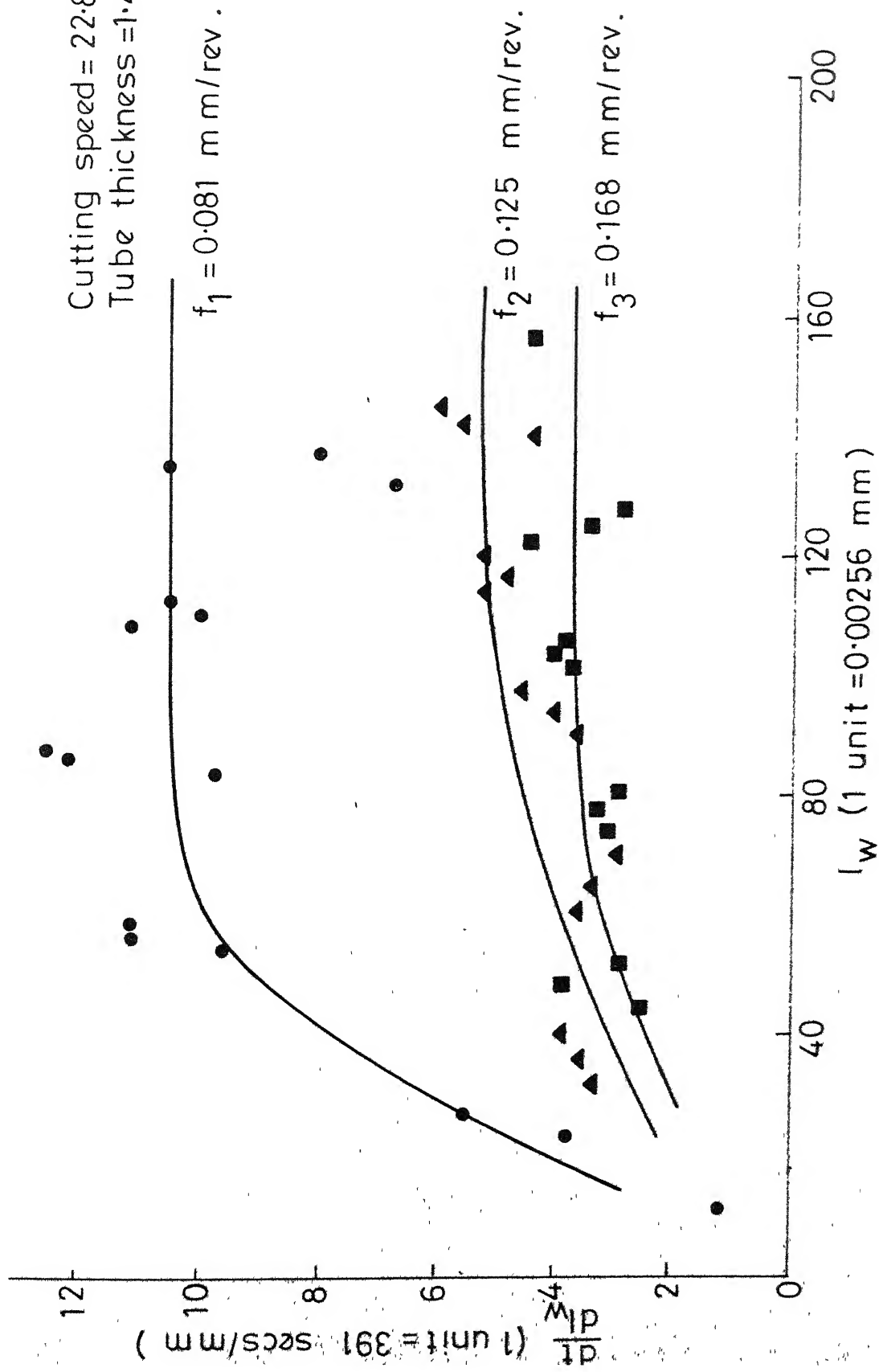


Fig. 5.1 Inverse wear-land growth rate curves for multifeed test I

Cutting speed = 22.8 m/min.
 Tube thickness = 1.40 mm

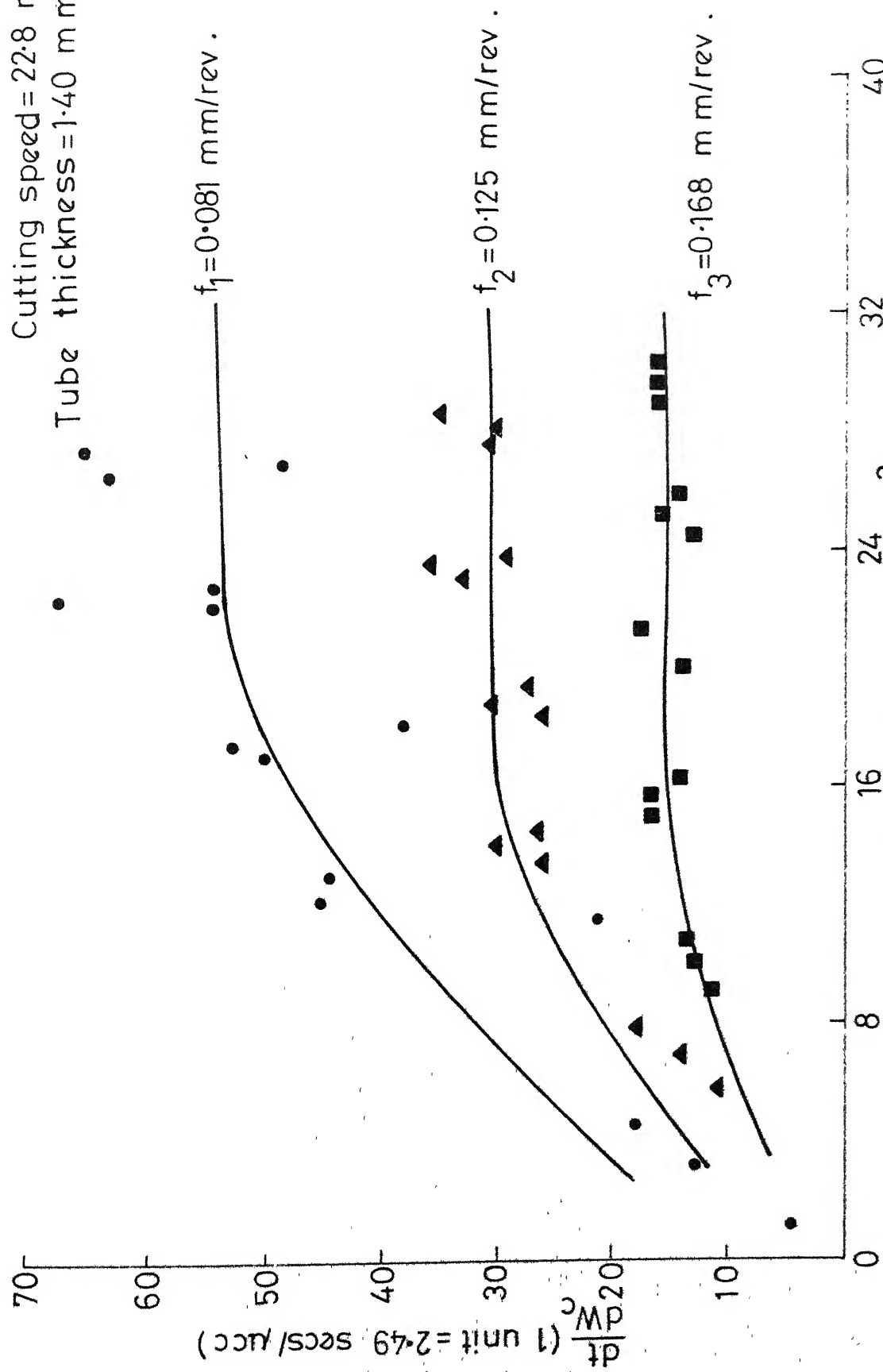


Fig. 5.2 Inverse crater volume growth rate curves for multifeed test 1

Cutting speed = 22.8 m/min.
 Tube thickness = 1.40 mm

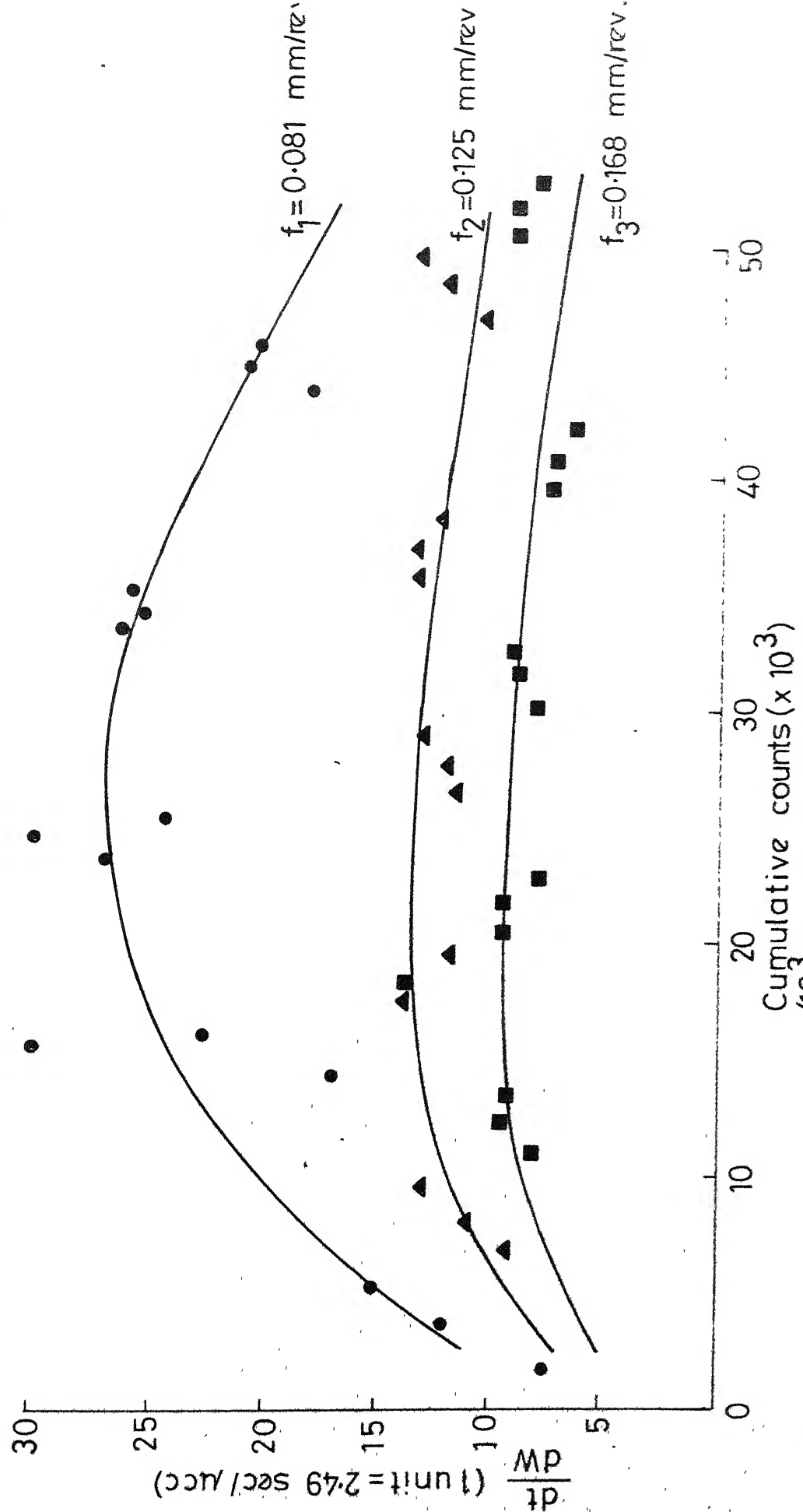


Fig. 5.3 Inverse total wear volume growth rate curves for multifeed test 1

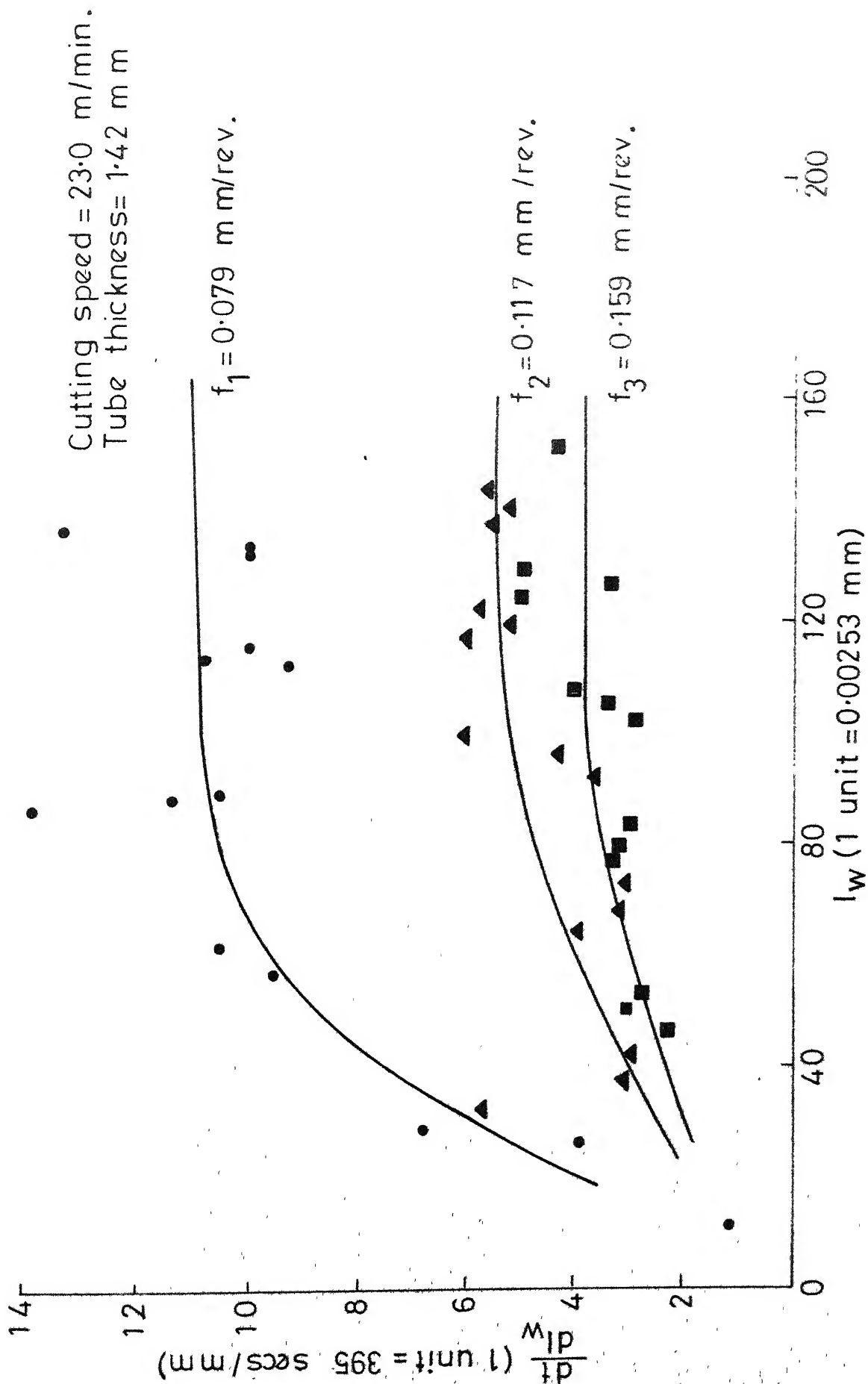


Fig. 5.4 Inverse wear-land growth rate curves for multifeed test 2

Cutting speed = 230m/min.
 Tube thickness = 1.42 mm

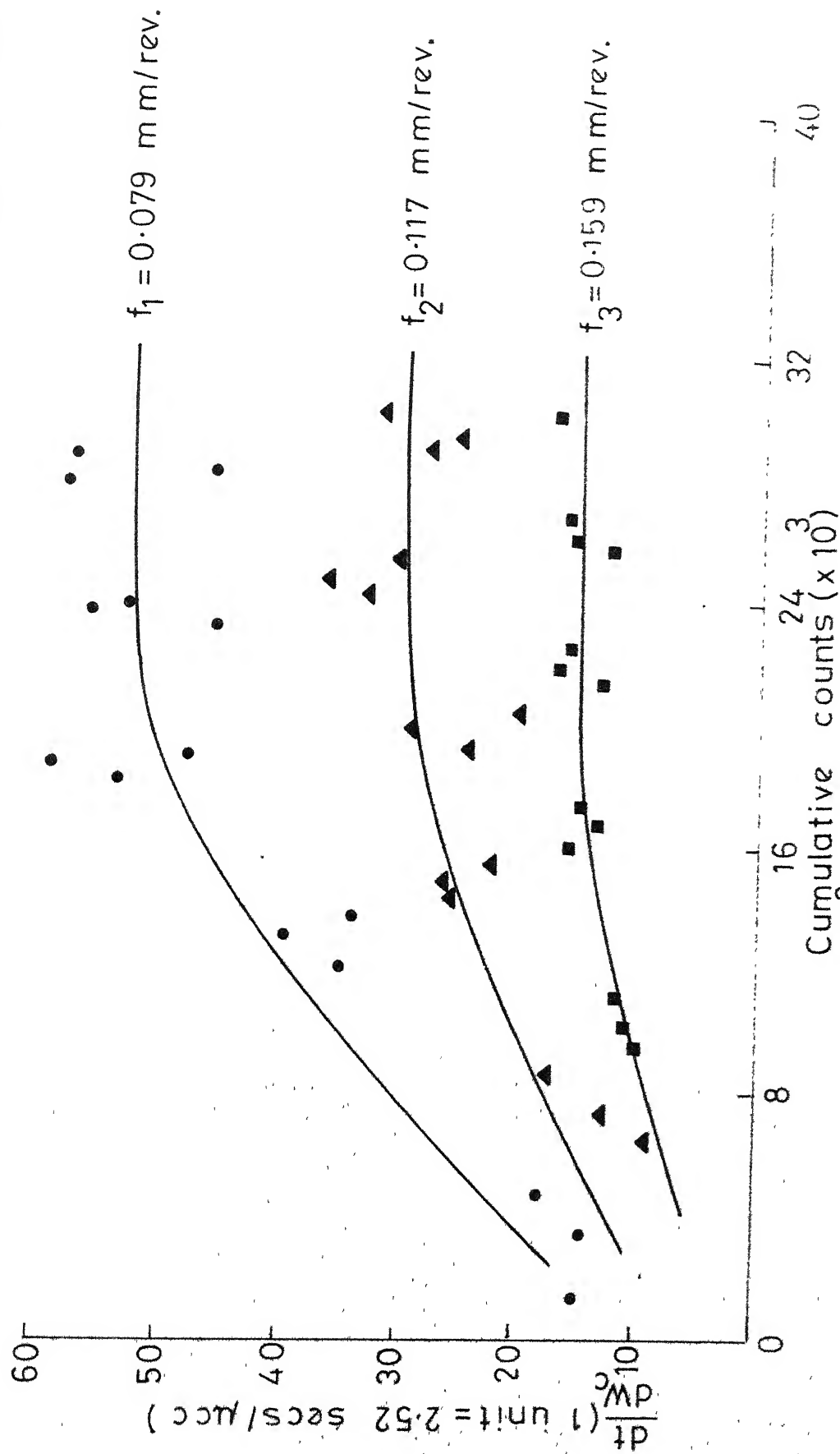


Fig. 5.5 Inverse crater wear volume growth rate curves for multifeed test 2

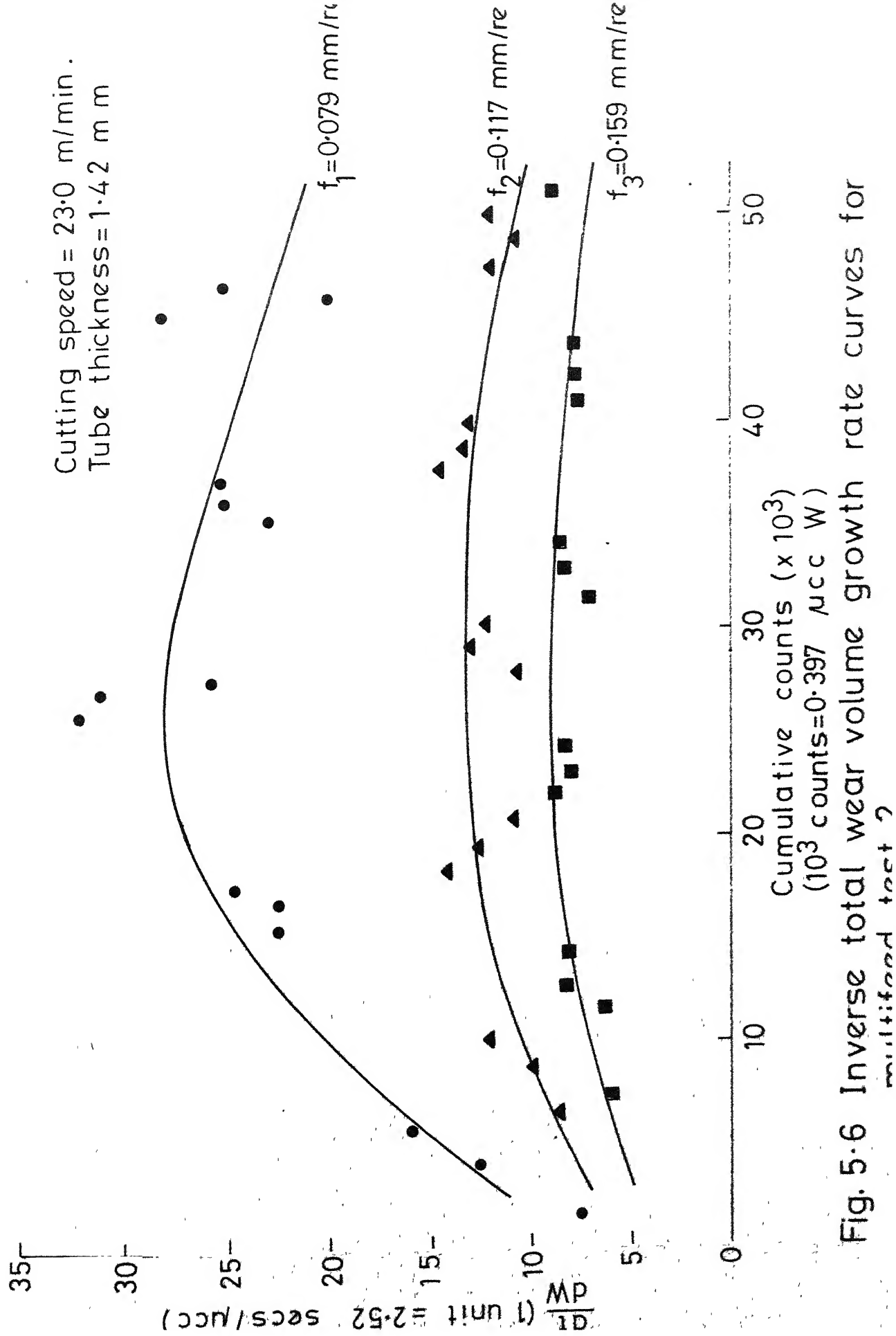


Fig. 5.6 Inverse total wear volume growth rate curves for
modified test ?

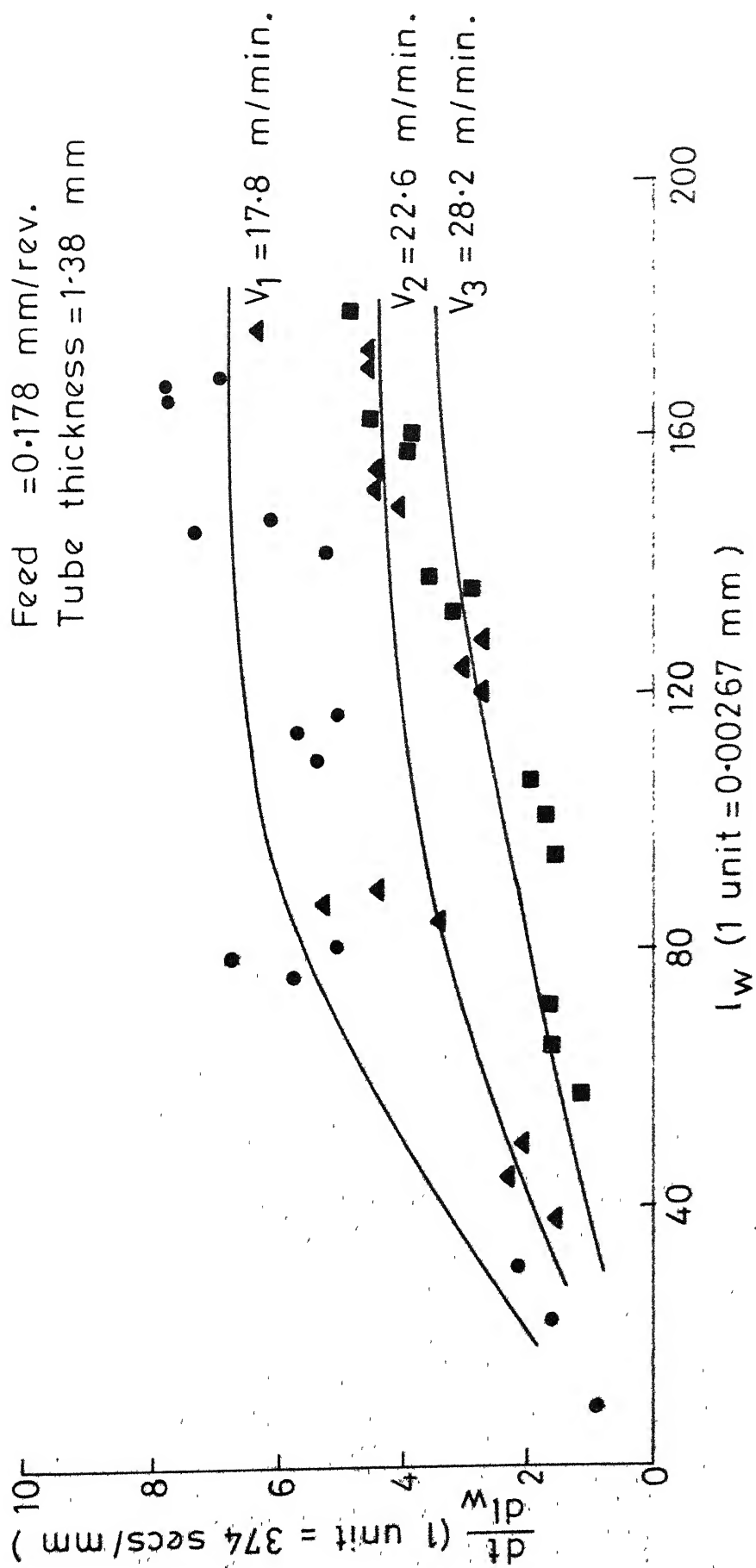


Fig.5.7 Inverse wear-land growth rate curves for multispeed test 1

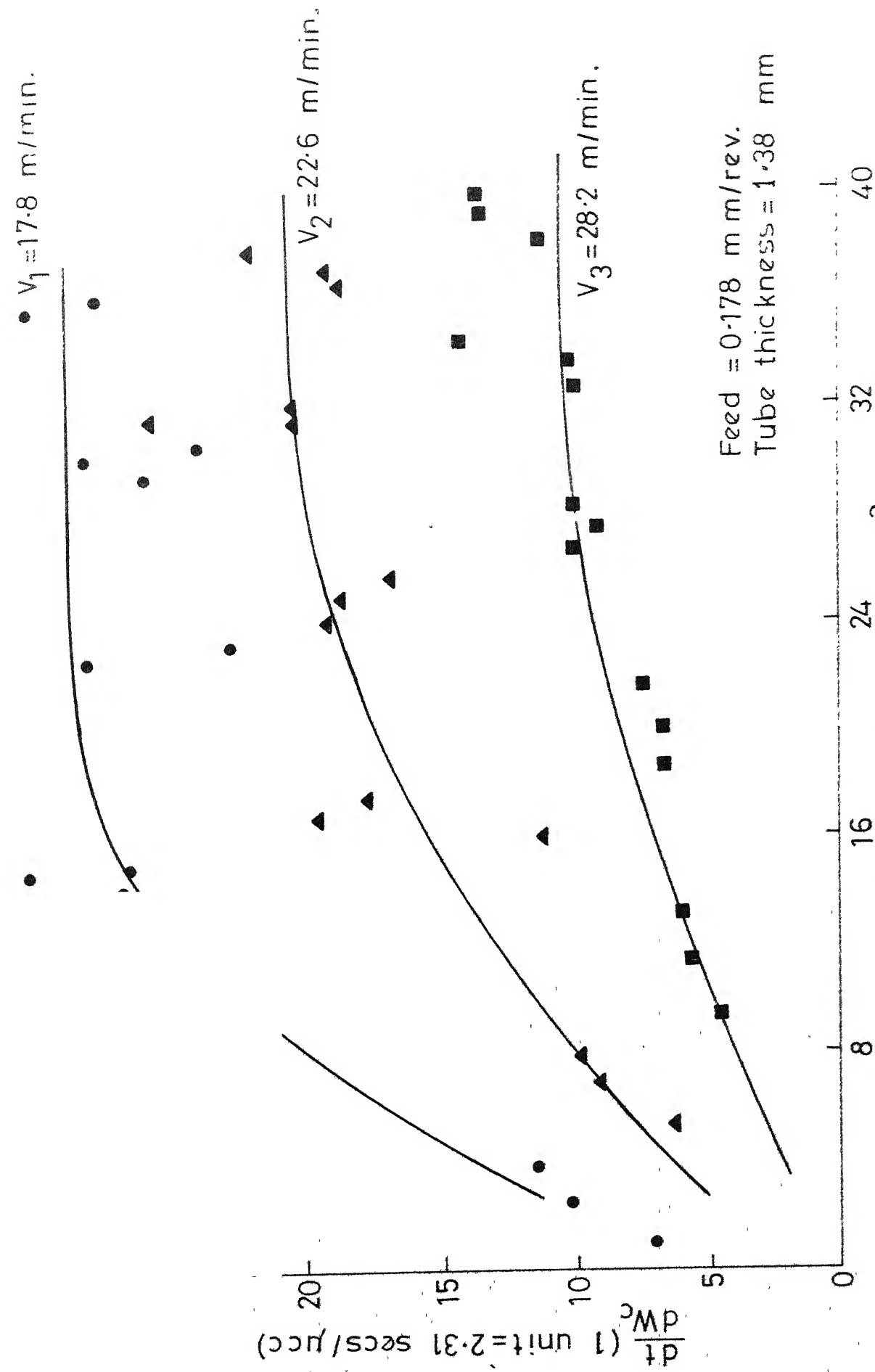
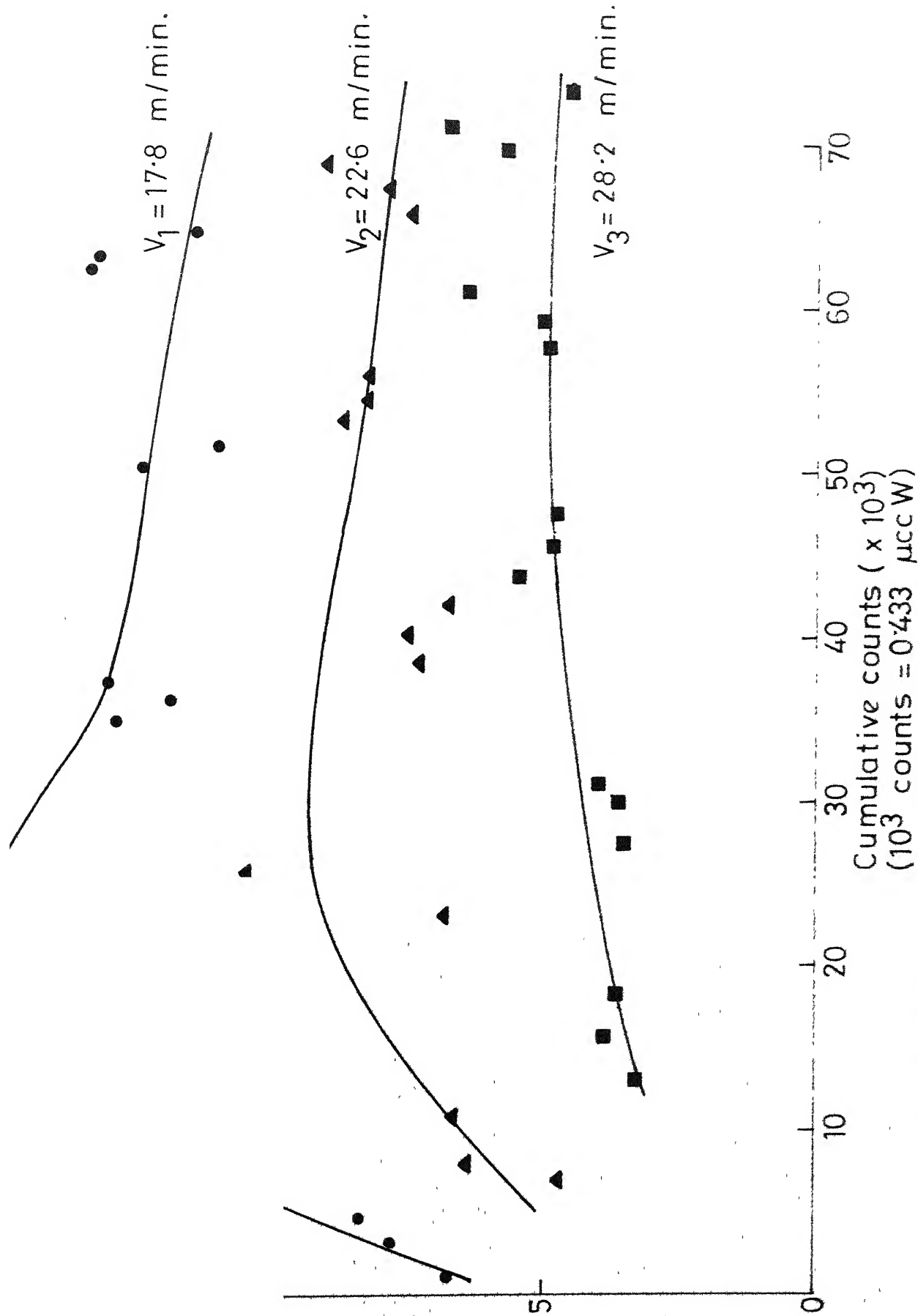


Fig. 5.8 Inverse crater wear volume growth rate curves for multispeed test 1



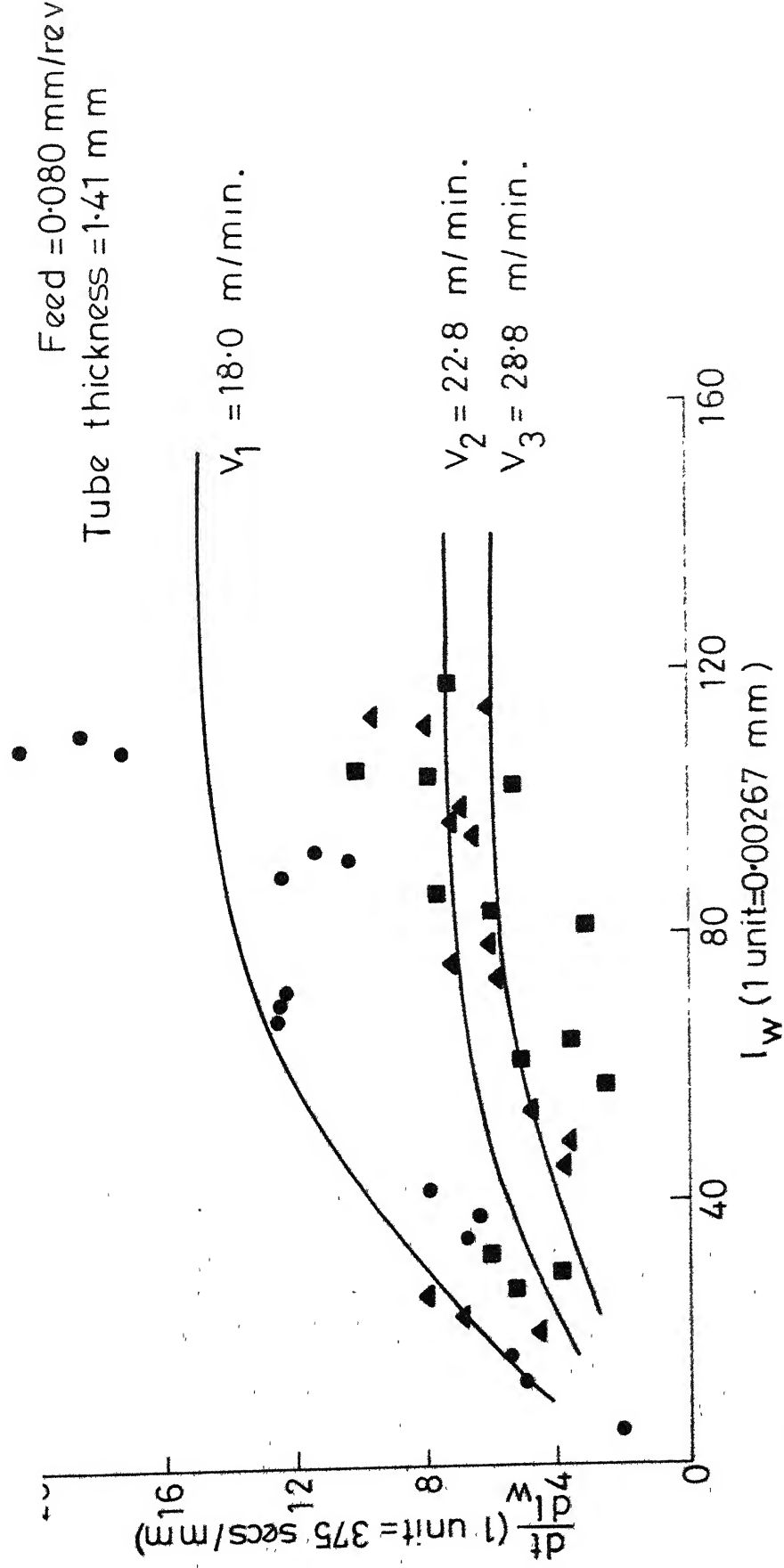
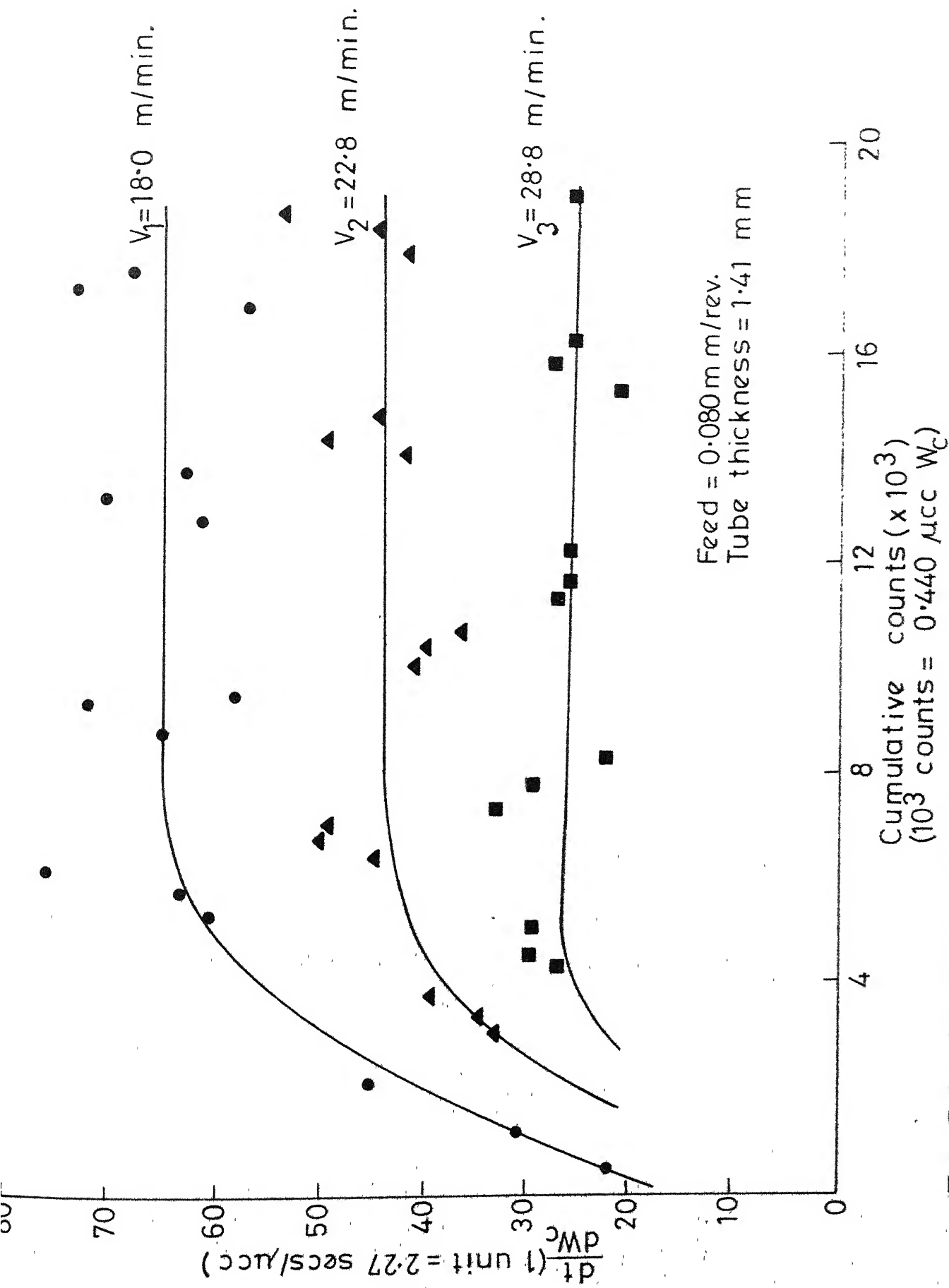


Fig. 5.10 Inverse wear-land growth rate curves for multispeed test 2



Feed = 0.080 mm/rev.

Tube thickness = 1.41 mm

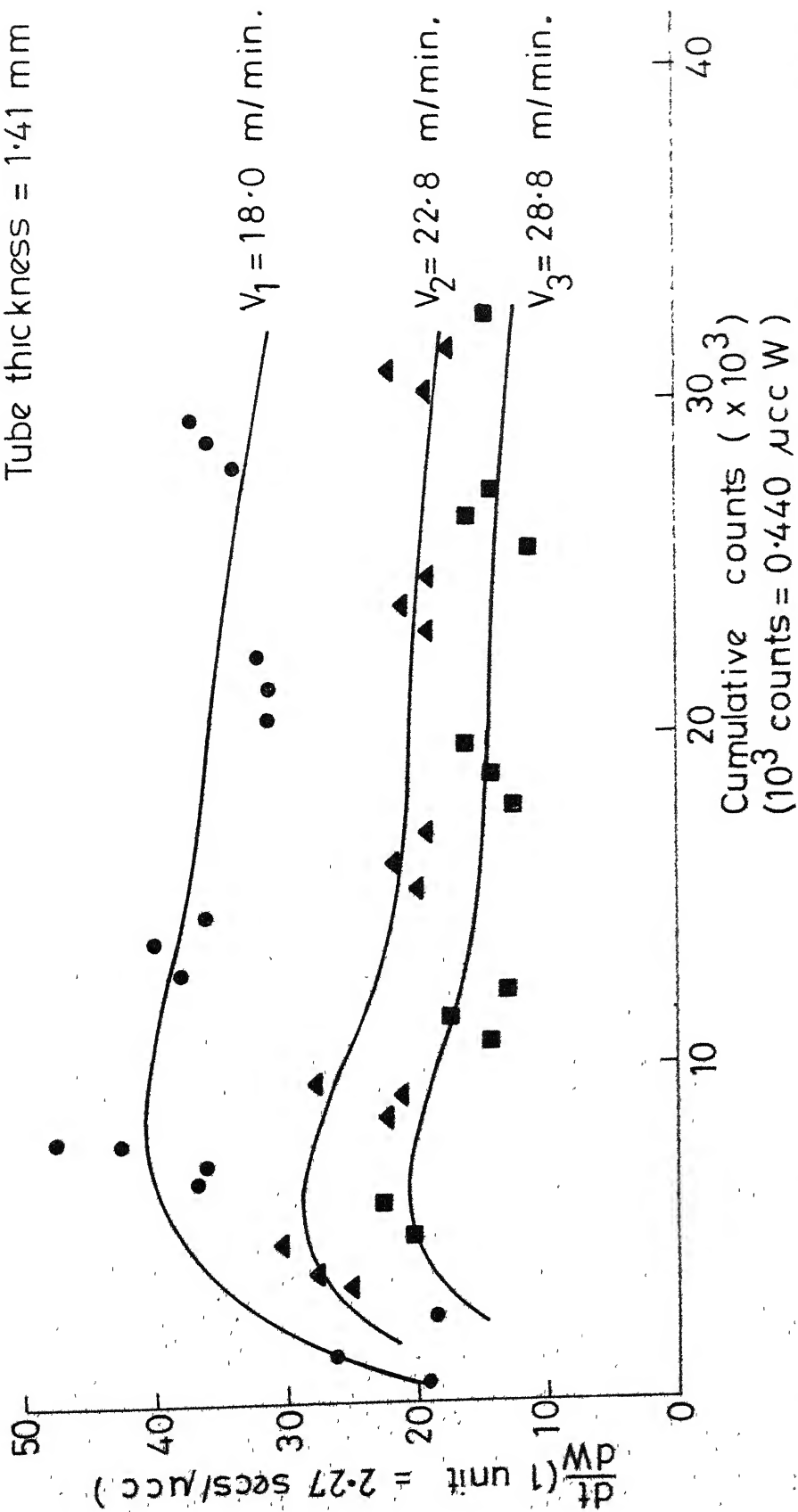


Fig. 5.12 Inverse total wear volume growth rate curves for multispeed test 2

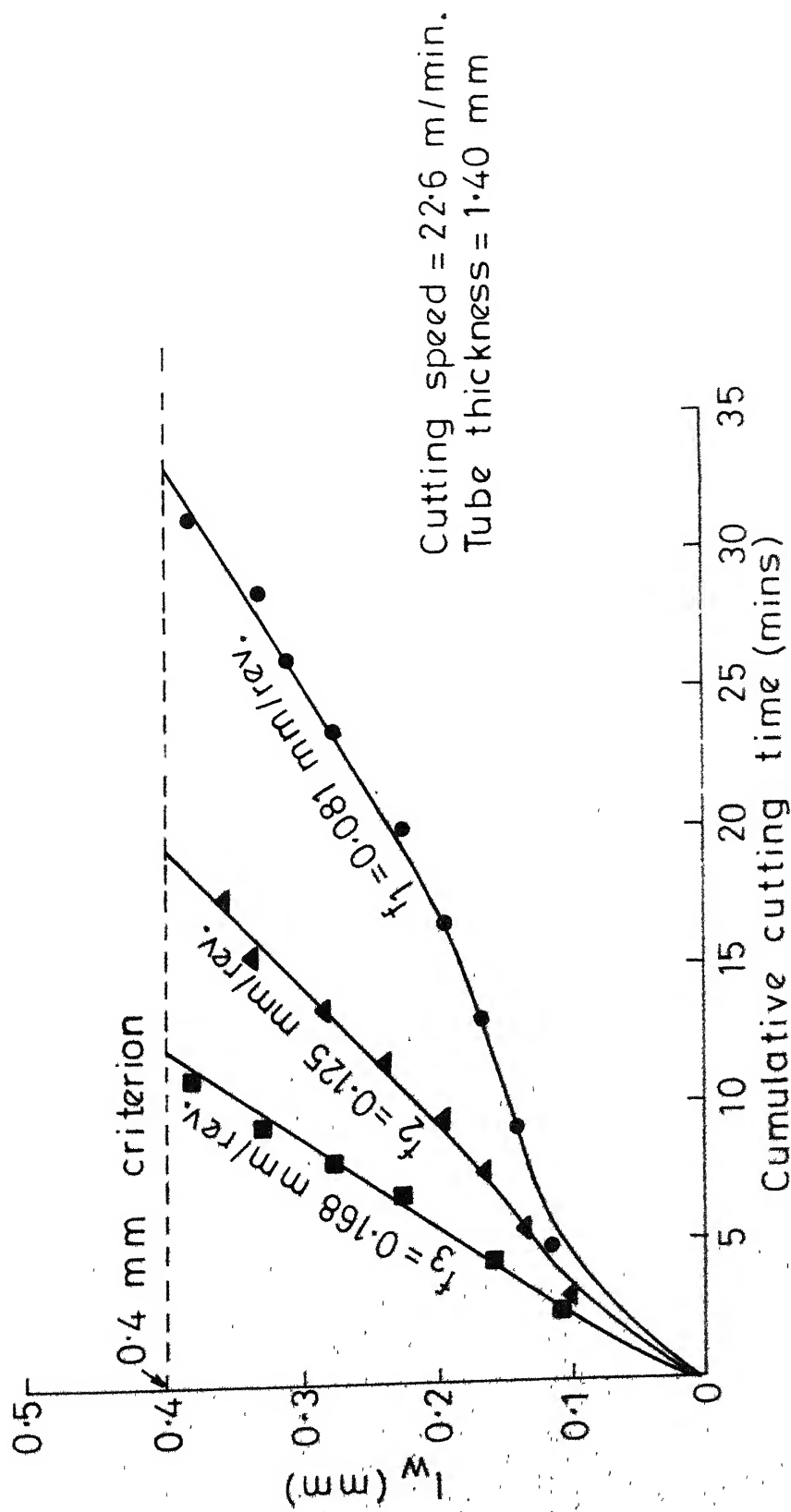


Fig. 5.13 Conventional measurements of wear-land growth in orthogonal cutting

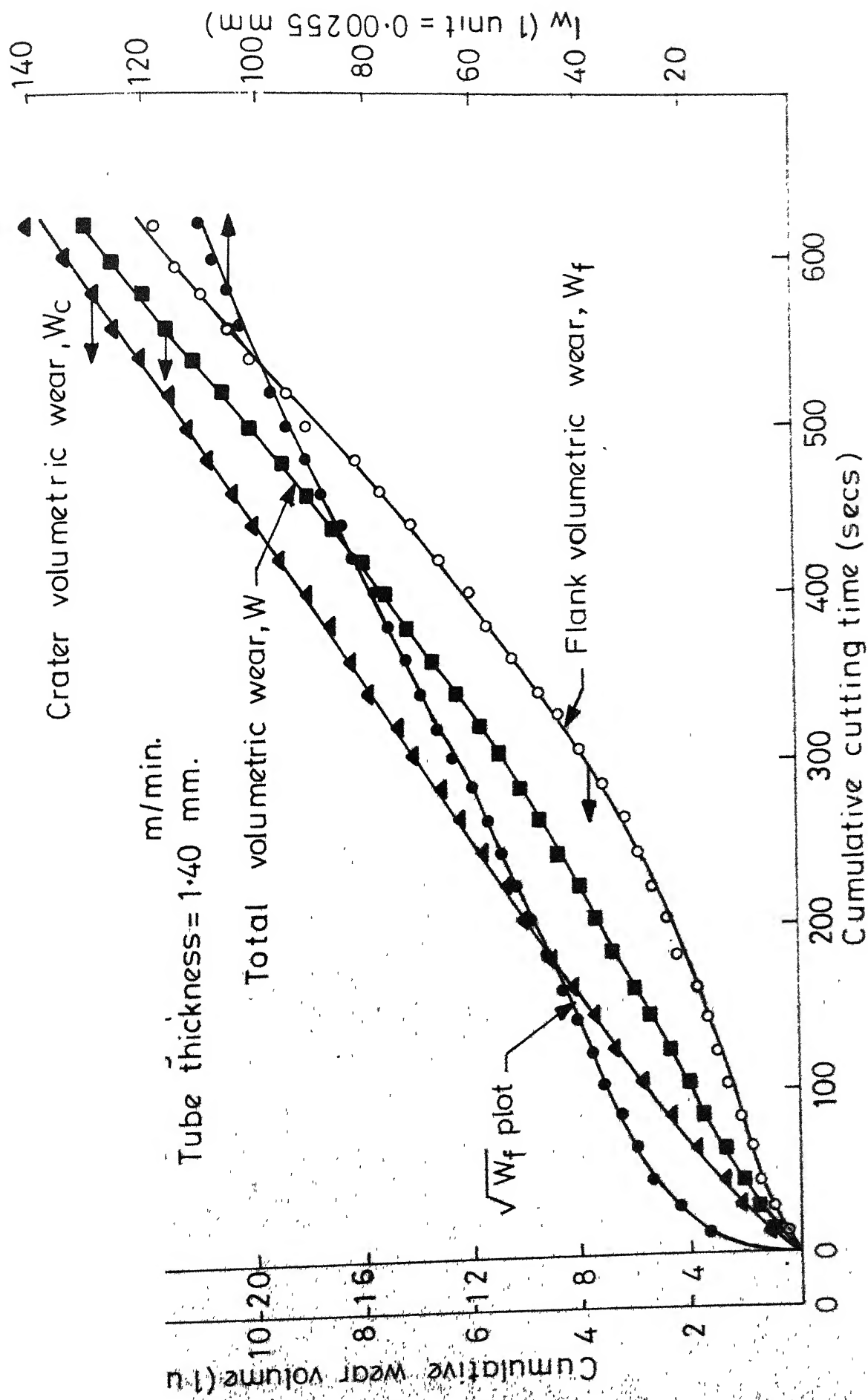


Fig. 5.14 Wear growth curves for the work material

Feed = 0.94 mm/rev.
 Cutting speed = 22.6 m/min.
 Tube thickness = 1.40 mm

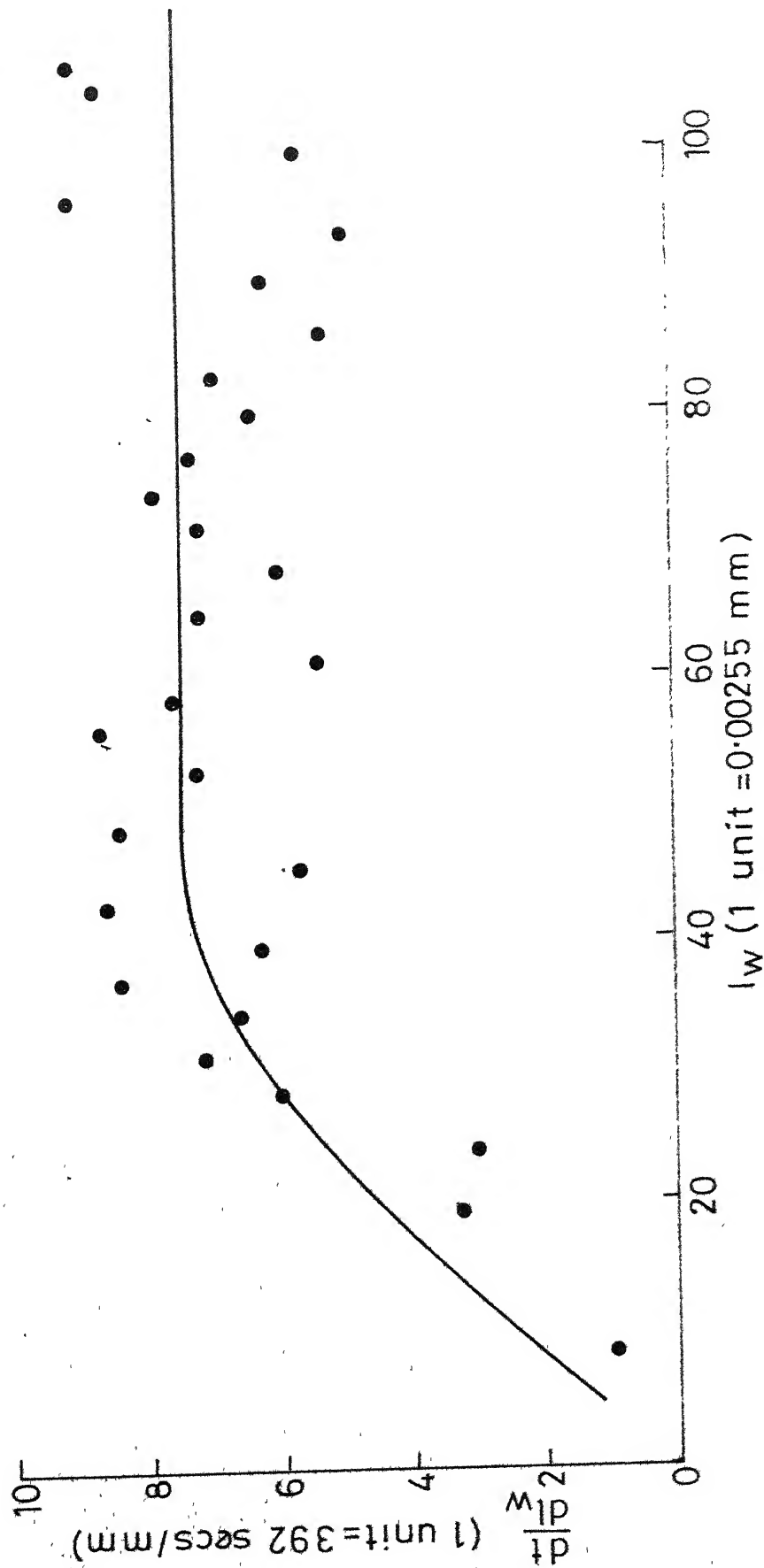


Fig. 5.15 Inverse wear land growth rate curve for single speed/feed test

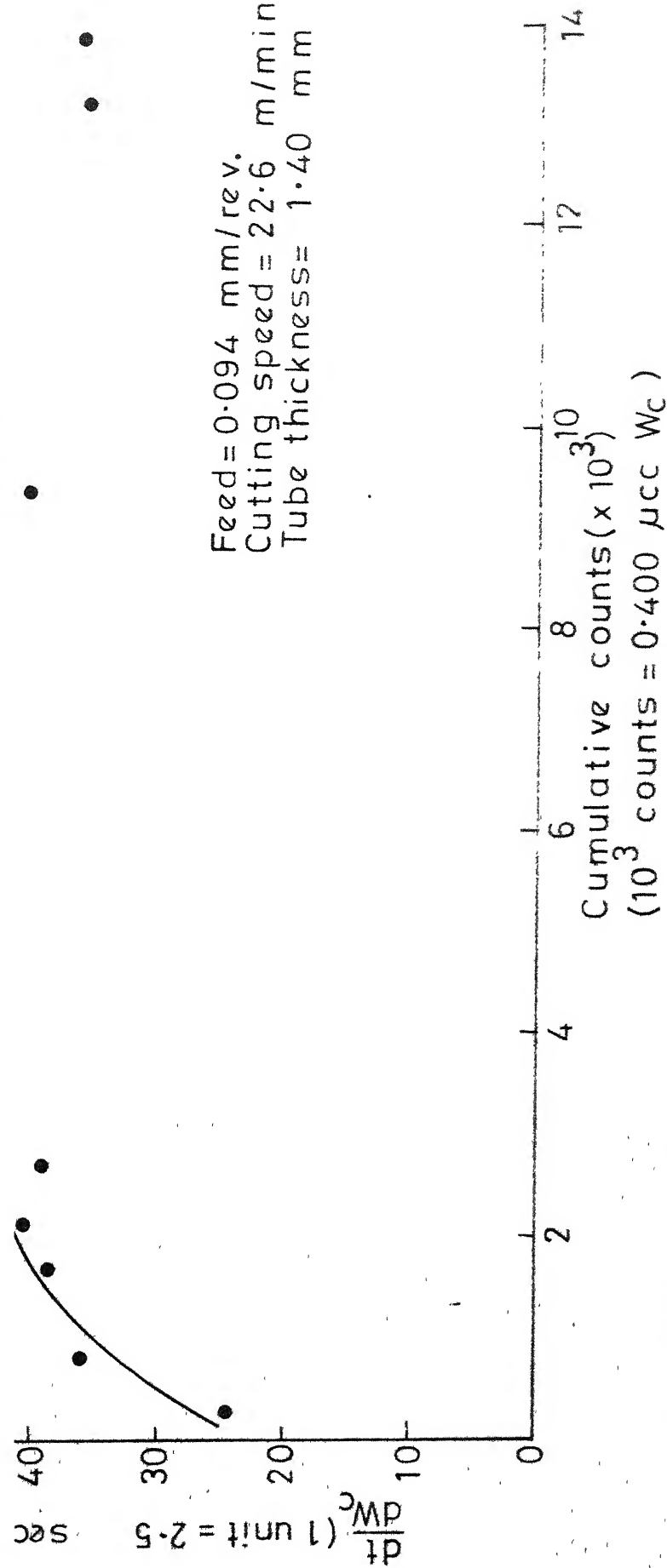


Fig. 5.16 Inverse crater wear volume growth rate curve for single speed/feed test

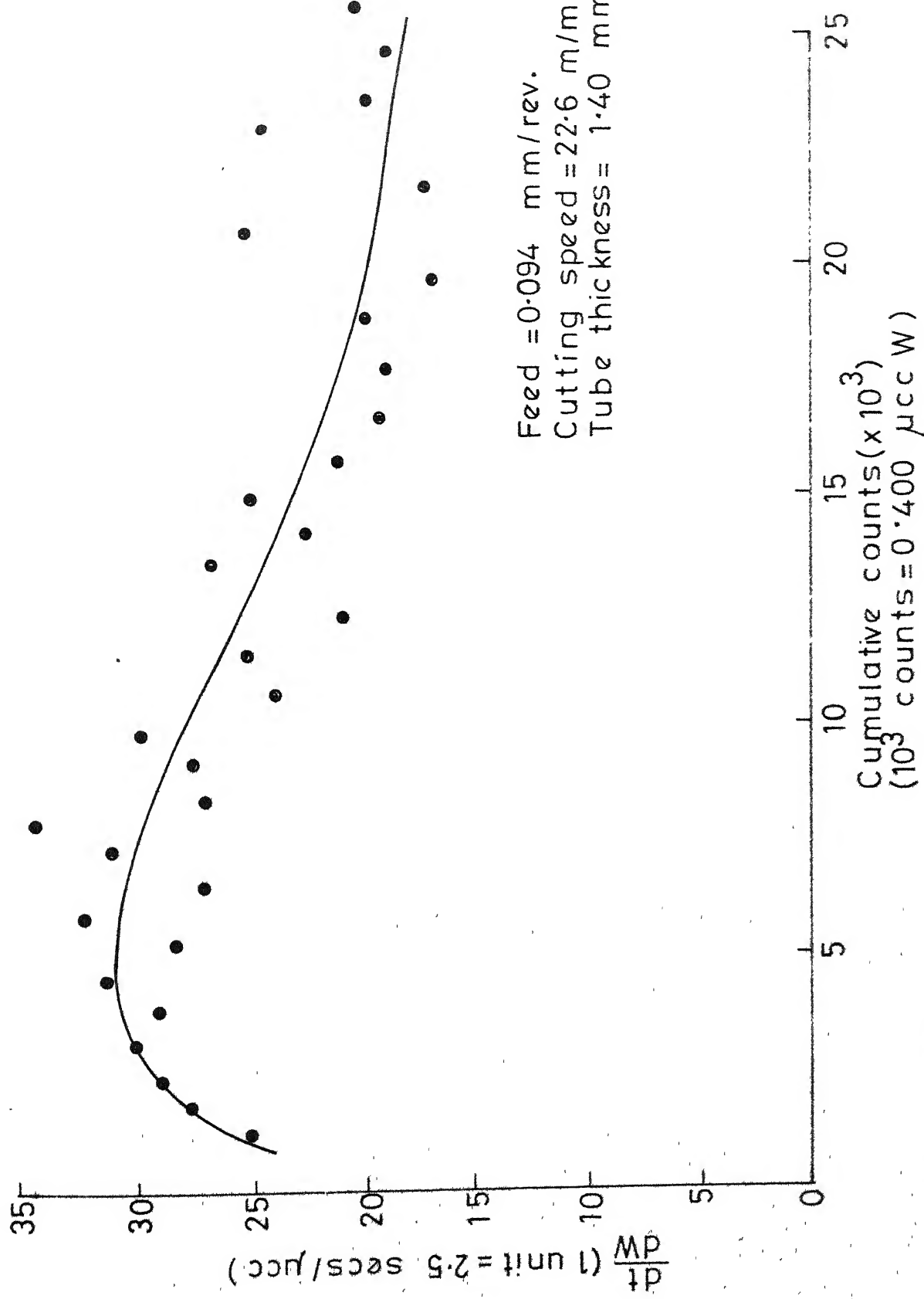
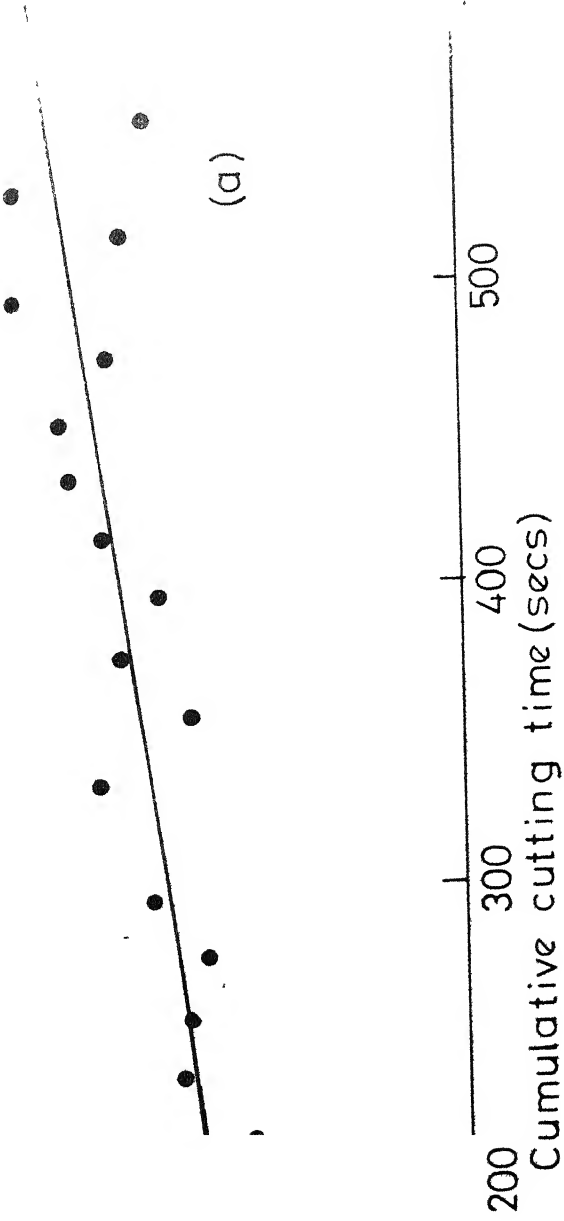


Fig. 5.17 Inverse total wear volume growth rate curve for single speed/feed test



Cumulative cutting time (secs)

100

200

300

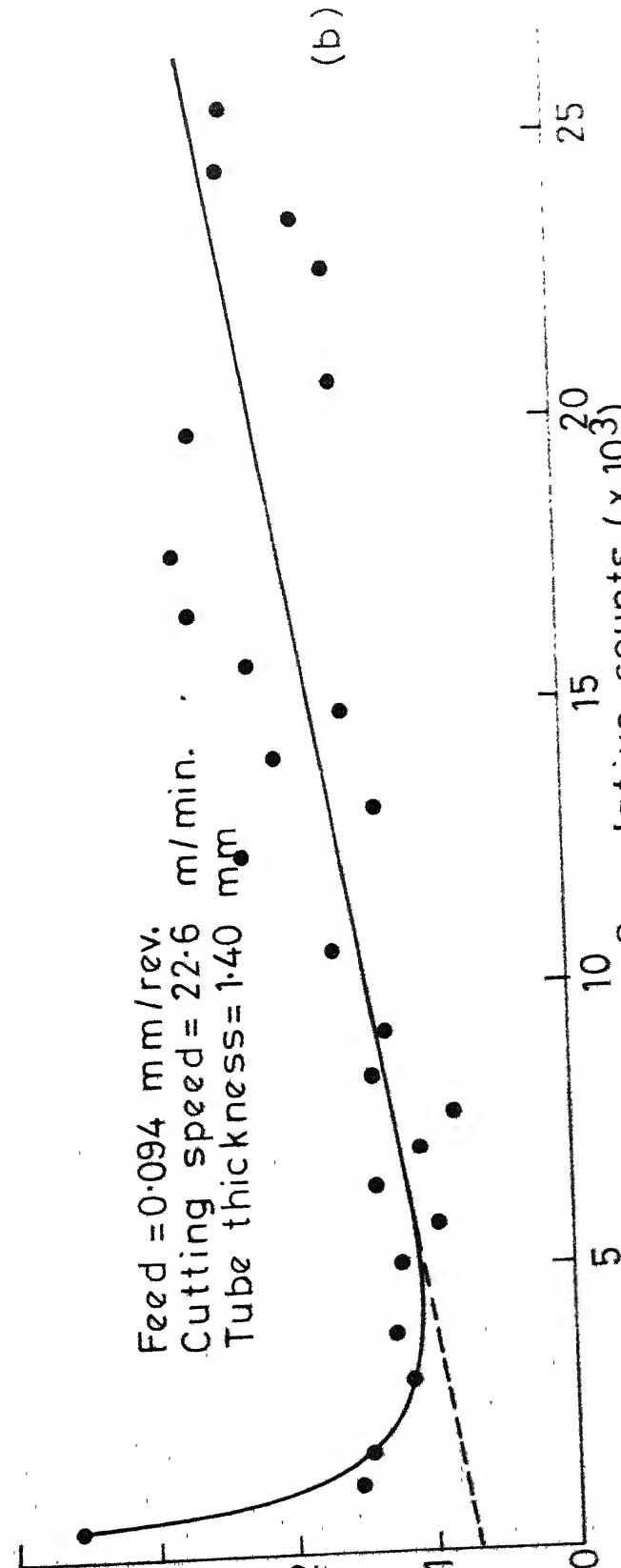
400

500

(a)

$\left(\frac{dV}{dt}\right)$ (1 unit = 0.160×10^{-3} m³/sec²)

Feed = 0.094 mm/rev.
Cutting speed = 22.6 m/min.
Tube thickness = 1.40 mm



(b)

Cumulative counts ($\times 10^3$)
(10³ counts = 0.400 μ cc W)

5

10

15

20

25

30

Fig. 5.18 (a) Wear-rate and (b) Square-of-wear-rate curves, for single speed/feed test

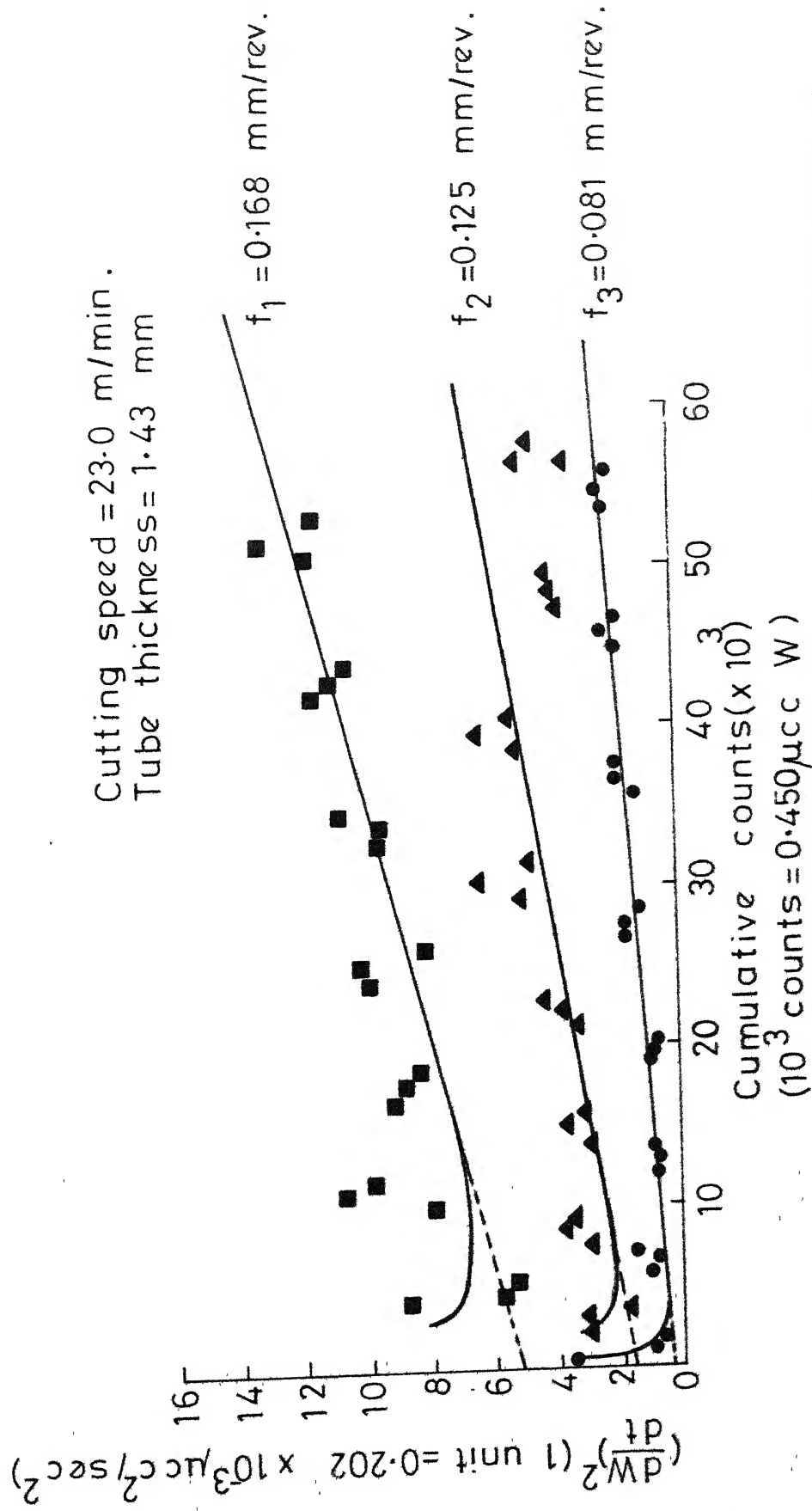


Fig. 5-19 Square-of-wear-rate curves for multifeed test 3

Cutting speed = 23.0 m/min.
 Tube thickness = 1.43 mm

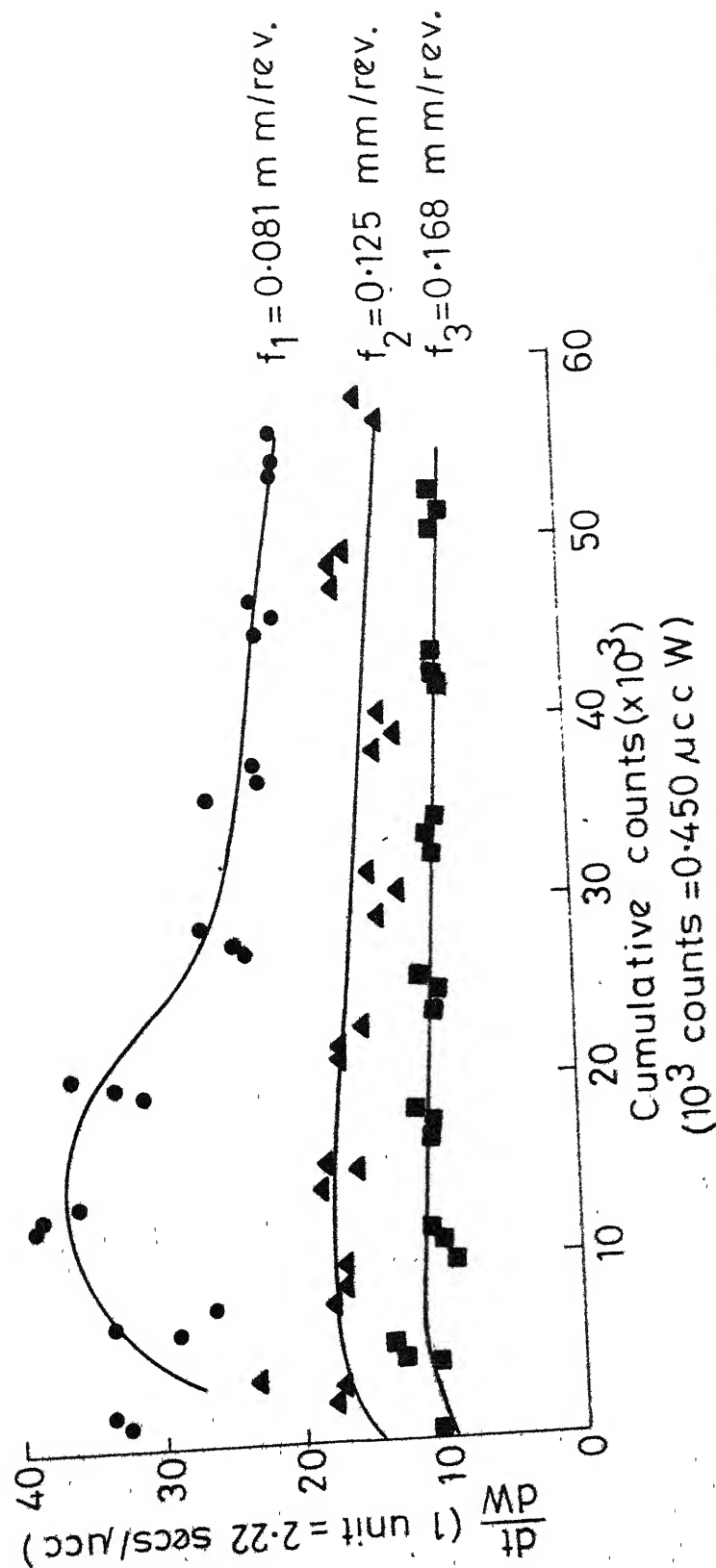


Fig. 5.20 Inverse total wear volume growth rate curves for multifeed test 3

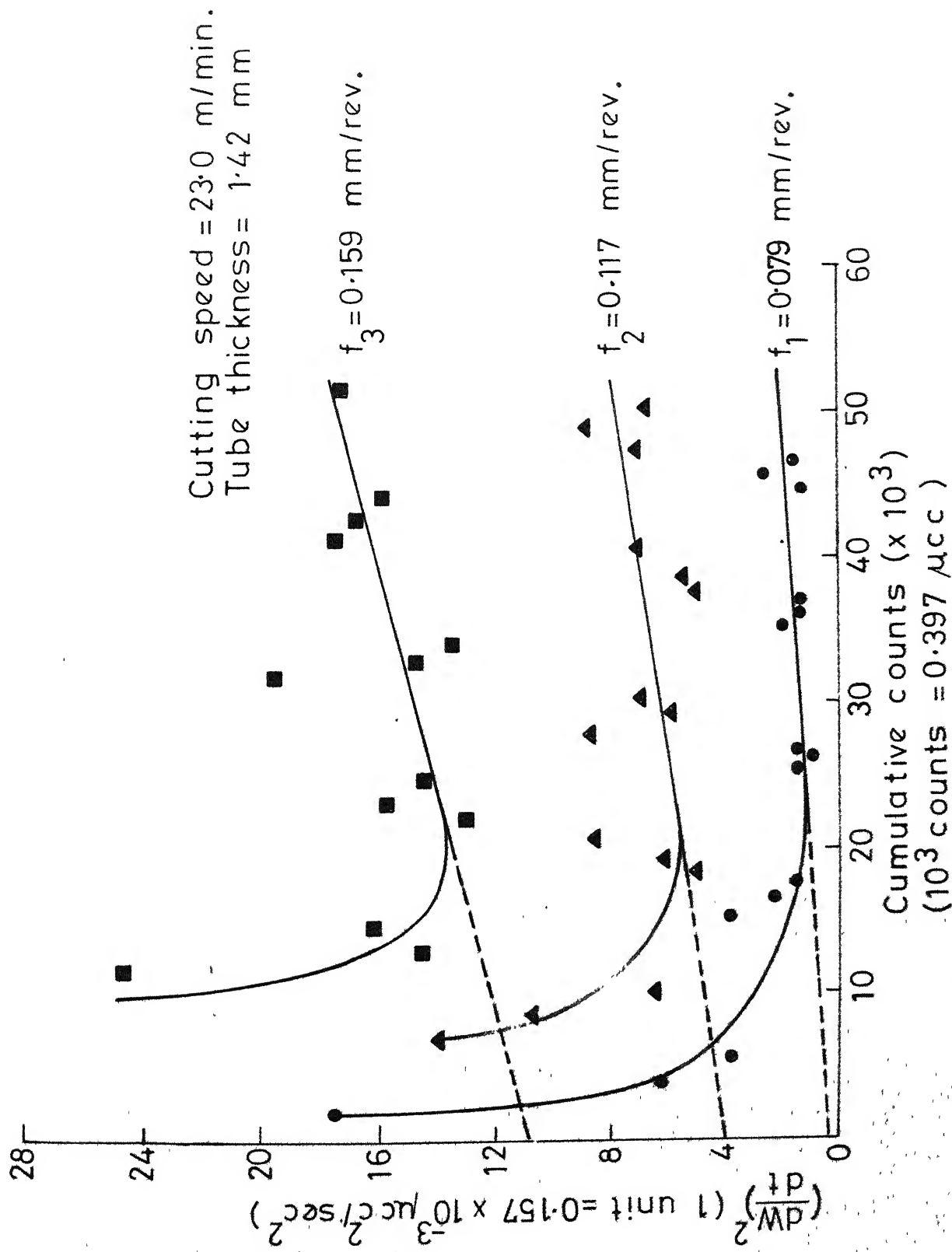


Fig. 5.21 Square-of-wear-rate curves for multifeed test-2

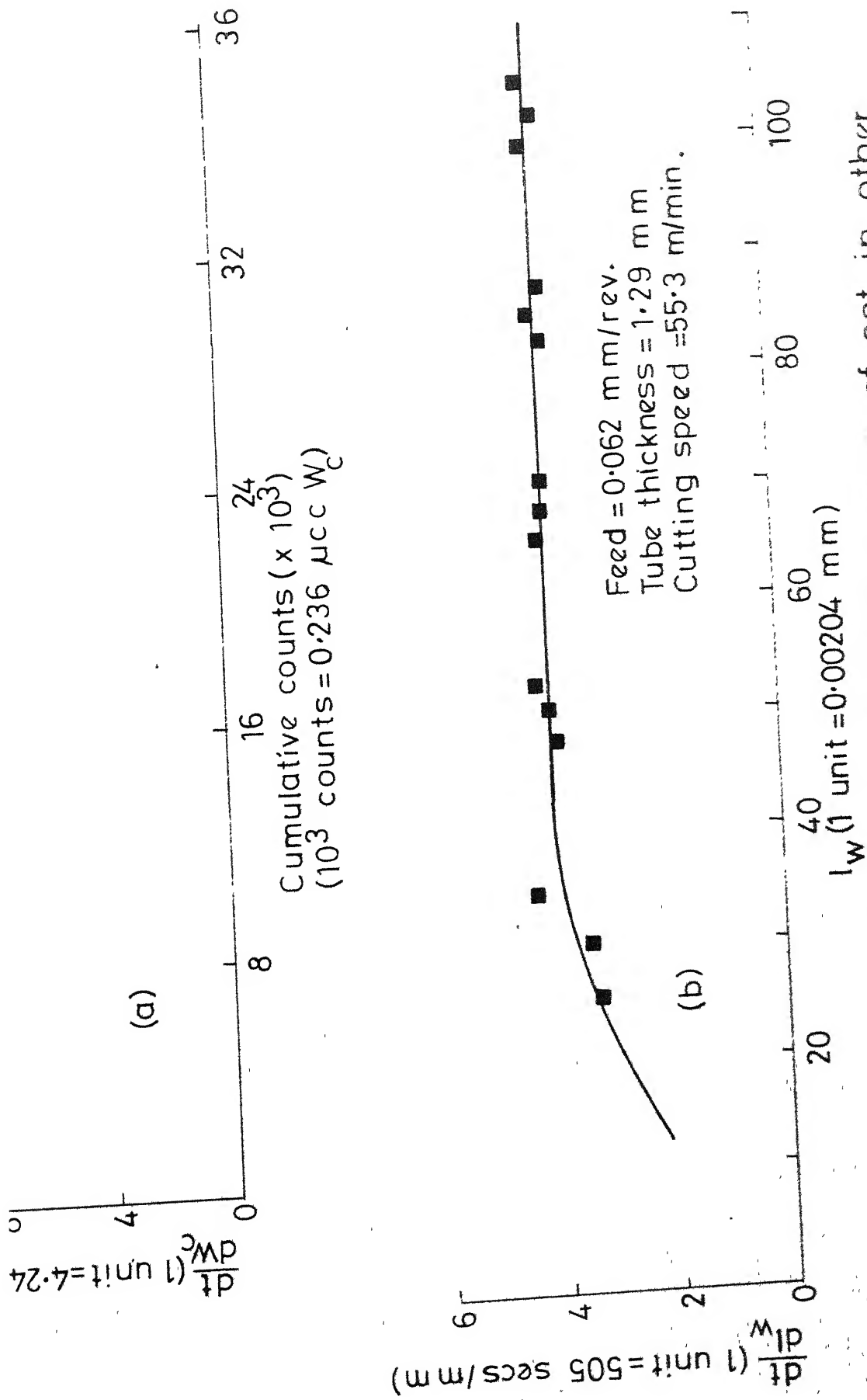


Fig. 5.22 Inverse wear growth rate curves of set in other test 1 (a) Crater wear volume (b) Flank wear-land.

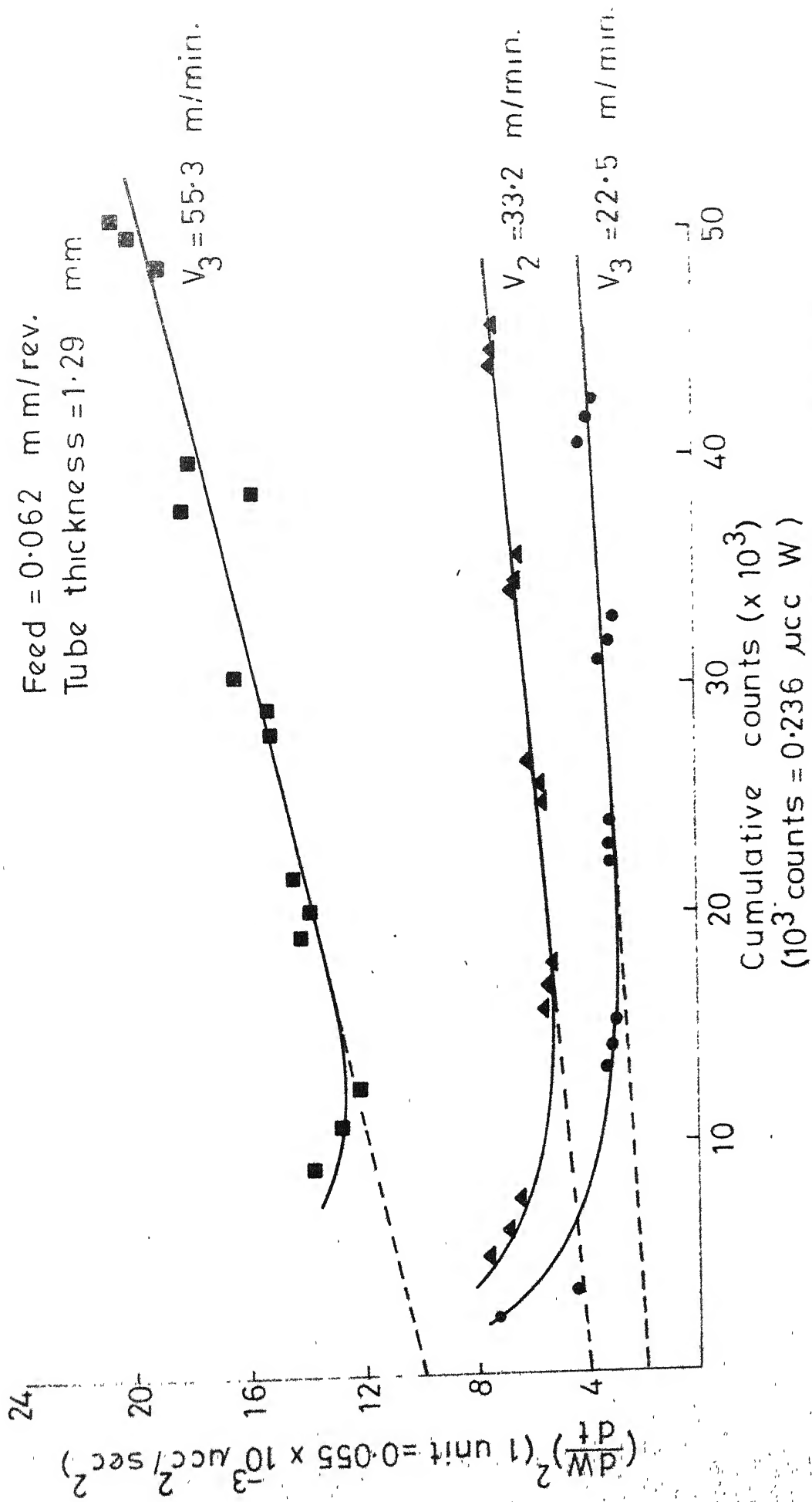


Fig. 5.23 Square-of-wear-rate curves for other test 1

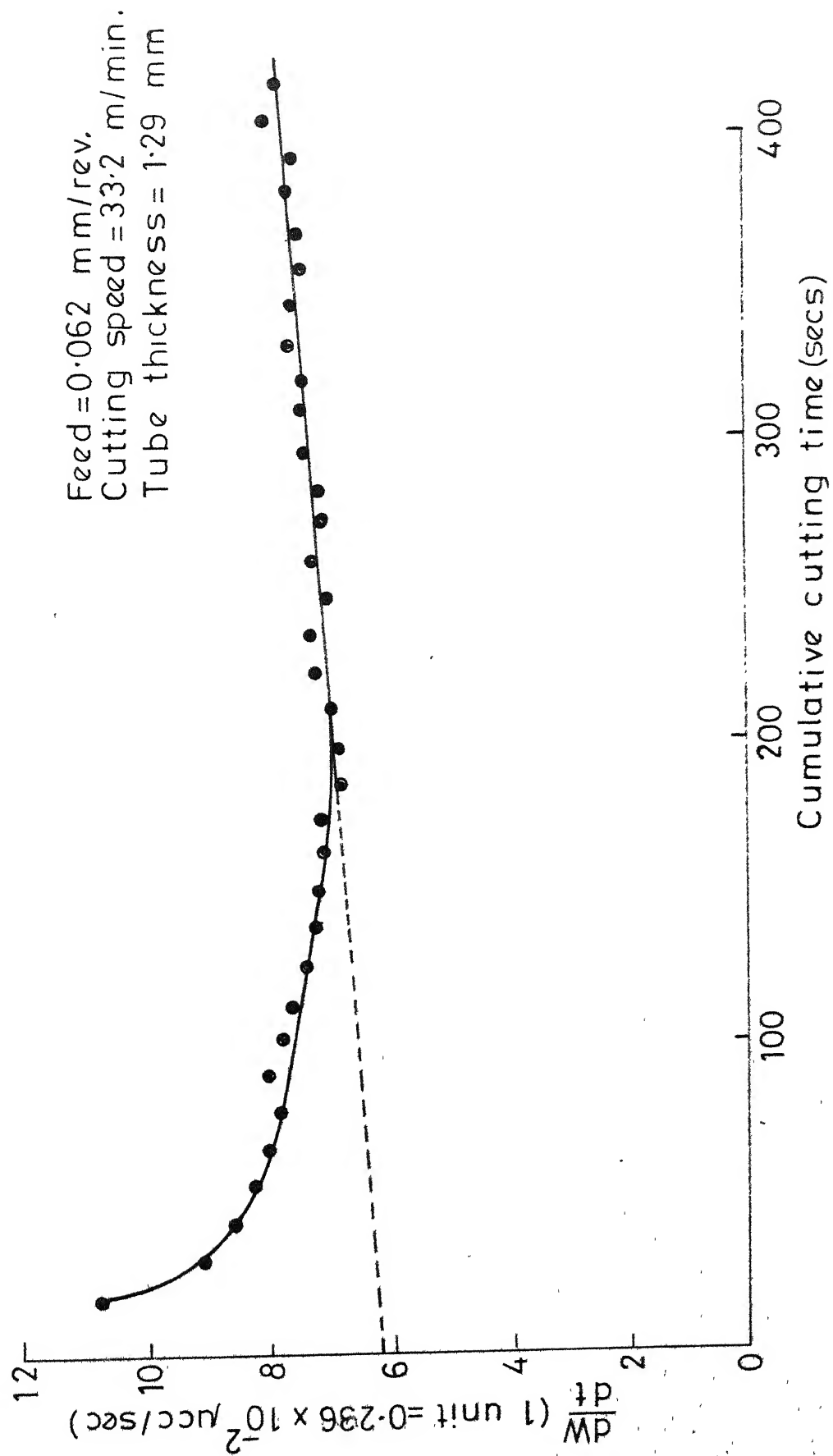


Fig. 5.24 Wear-rate curve for other test 2

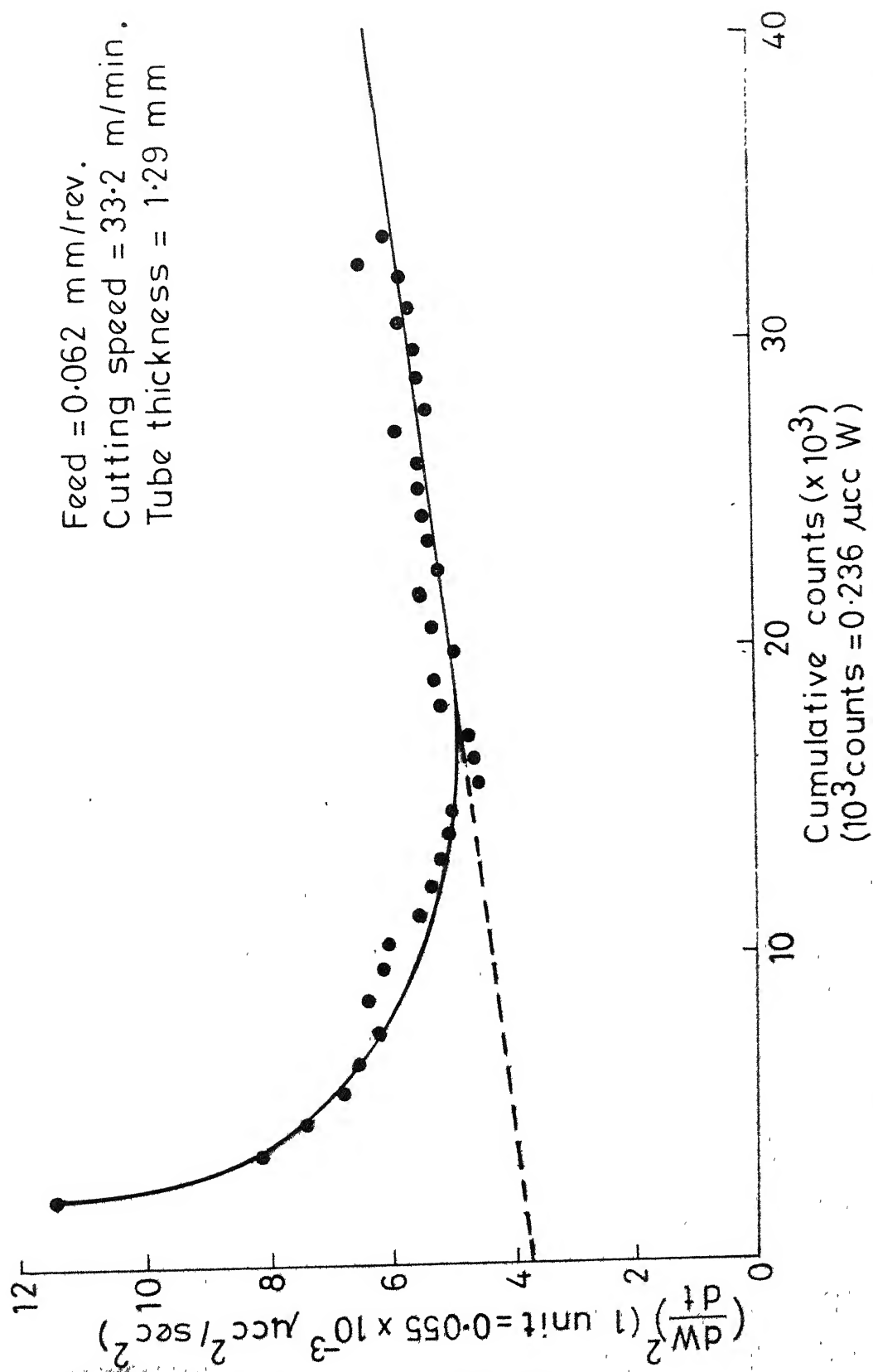


Fig. 5.25 Square-of-wear-rate curves for other test 2

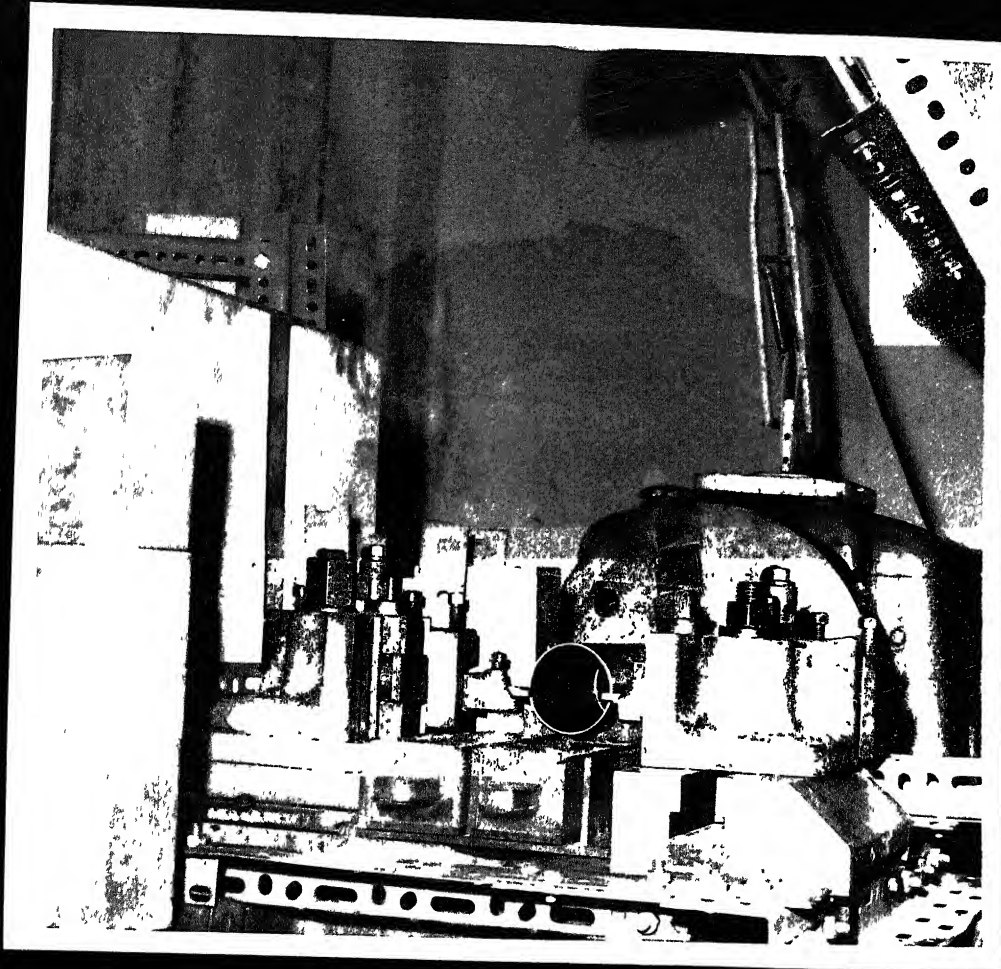


PLATE : General View of the Experimental Set-up.

Date Slip **A 54003**

[illegible]

ME-1977-M-DAT-INV